© 2017. Published by The Company of Biologists Ltd | Development (2017) 144, 601-611 doi:10.1242/dev.139873

STEM CELLS AND REGENERATION

RESEARCH ARTICLE

Retinoic acid receptor regulation of epimorphic and homeostatic regeneration in the axolotl

Matthew Nguyen[1], Pankhuri Singhal[1], Judith W. Piet[2], Sandra J. Shefelbine[2], Malcolm Maden[3], S. Randal Voss[4,5] and James R. Monaghan[1,*]

ABSTRACT

Salamanders are capable of regenerating amputated limbs by generating a mass of lineage-restricted cells called a blastema. Blastemas only generate structures distal to their origin unless treated with retinoic acid (RA), which results in proximodistal (PD) limb duplications. Little is known about the transcriptional network that regulates PD duplication. In this study, we target specific retinoic acid receptors (RARs) to either PD duplicate (RA treatment or RARγ agonist) or truncate (RARβ antagonist) regenerating limbs. RARE-EGFP reporter axolotls showed divergent reporter activity in limbs undergoing PD duplication versus truncation, suggesting differences in patterning and skeletal regeneration. Transcriptomics identified expression patterns that explain PD duplication, including upregulation of proximal homeobox gene expression and silencing of distal-associated genes, whereas limb truncation was associated with disrupted skeletal differentiation. RARβ antagonism in uninjured limbs induced a loss of skeletal integrity leading to long bone regression and loss of skeletal turnover. Overall, mechanisms were identified that regulate the multifaceted roles of RARs in the salamander limb including regulation of skeletal patterning during epimorphic regeneration, skeletal tissue differentiation during regeneration, and homeostatic regeneration of intact limbs.

KEY WORDS: Regeneration, Retinoic acid, RAR, Limb, Patterning, Chondrogenesis

INTRODUCTION

Urodele amphibians (salamanders) are capable of regenerating amputated limbs and tails throughout life by recruiting cells juxtaposed to the amputation plane to migrate distally (towards the hand) and proliferate into a mass of lineage-restricted cells called a blastema (Kragl et al., 2009; Monaghan and Maden, 2012a). Blastemas only regenerate structures distal to their origin, known as the 'rule of distal transformation', using positional cues provided by cells proximal to the amputation plane (Ludolph et al., 1990; Maden, 1980; Stocum and Thoms, 1984). Young blastemal cells are in a state of cellular plasticity, which allows them to adopt distal positional values (McCusker et al., 2014; McCusker and Gardiner, 2013; Roensch et al., 2013). Young distal limb blastema cells can be reprogrammed with supplemental retinoic acid (RA) to a proximal fate (Maden, 1982), posterior fate (Kim and Stocum, 1986; Stocum and Thoms, 1984) and ventral fate (Ludolph et al., 1990), which will not occur in uninjured limbs (McCusker et al., 2014; Niazi et al., 1985) or after redifferentiation has commenced (Niazi et al., 1985). Despite the power of this experimental approach for understanding the role of RA during regeneration and how positional identity is established and maintained, little is known about the transcriptional network that regulates positional information.

RA is a molecule with pleiotropic functions that is vital during vertebrate development for regulating embryo patterning, cell differentiation, and organogenesis (Clagett-Dame and DeLuca, 2002; Duester, 2013; Marlétaz et al., 2006). RA signaling controls developmental processes by regulating gene transcription through the activation of retinoic acid receptors (RARα, RARβ and RARγ). RARs heterodimerize to retinoid X receptors (RXRs) and, together, these transcriptional complexes bind to retinoic acid DNA response elements (RAREs) located near RA target genes (Chambon, 1996). RAR/RXR complexes work as transcriptional repressors with no ligand and as activators in the presence of RA ligand (Rochette-Egly and Germain, 2009). Limiting RA concentration, inhibiting RAR signaling, or inhibiting RA metabolism has detrimental effects on limb development in chicks (Roselló-Díez et al., 2011; Stratford et al., 1996), zebrafish (Grandel et al., 2002) and mammals (Dranse et al., 2011; Lohnes et al., 1994; Niederreither et al., 2002; Sandell et al., 2012, 2007; Williams et al., 2009; Yashiro et al., 2004). The role of RA during limb regeneration is less clear (Blum and Begemann, 2013), although several lines of evidence support an active role. RA is present in regenerating limbs (Scadding and Maden, 1994) and RA-reporter axolotls show RA signaling in regenerating limbs (Monaghan and Maden, 2012b). Genes that regulate RA signaling are expressed in regenerating frog limbs (McEwan et al., 2011) and salamanders including *Rdh10* (Monaghan et al., 2012), *Raldh1* (Knapp et al., 2013), *Raldh3* (Monaghan et al., 2012), *Rarα* (Ragsdale et al., 1989) *Rarβ* (Carter et al., 2011; Giguère et al., 1989) and *Rarγ* (Hill et al., 1993; Ragsdale et al., 1989; Voss et al., 2015). Also, *Raldh* inhibition blocks axolotl limb regeneration (Maden, 1998; Scadding, 2000), and also epimorphic fin zebrafish regeneration (Blum and Begemann, 2012), and excess RA induces duplicated patterning during *Xenopus* hindlimb regeneration (Cuervo and Chimal-Monroy, 2013) as it does in salamanders.

RA will reprogram regenerating limbs up to the early/mid limb bud stage in axolotl salamanders, but generates hypomorphic limbs when treated during development. Both phenotypes can be observed simultaneously in axolotls because hindlimbs emerge late in development, when forelimbs have already completely differentiated (Scadding and Maden, 1986). Hypomorphic regeneration also occurs when RA is added to limbs after the early/mid bud stage, suggesting that RA signaling cannot influence

[1]Department of Biology, Northeastern University, Boston, MA 02115, USA. [2]Mechanical and Industrial Engineering, Northeastern University, Boston, MA 02115, USA. [3]Department of Biology and UF Genetics Institute, University of Florida, Gainesville, FL 32611, USA. [4]Department of Biology, University of Kentucky, Lexington, KY 40506, USA. [5]Spinal Cord and Brain Injury Research Center, University of Kentucky, College of Medicine, Lexington, KY 40506, USA.

*Author for correspondence (j.monaghan@neu.edu)

M.M., 0000-0001-7178-5309; J.R.M., 0000-0002-6689-6108

Received 16 May 2016; Accepted 30 December 2016

Development (2017) 144, 601-611 doi:10.1242/dev.139873

the PD axis outside the developmentally plastic phase of the early blastema (Maden, 1983; Niazi et al., 1985). Our previous work using reporter-based analysis supports this hypothesis because RA reporter activity is different between developing and regenerating limbs. Furthermore, adding excess RA during the early bud stage of regeneration (5 days post amputation) induced RA reporter activity in blastema connective tissue fibroblasts (Monaghan and Maden, 2012b), the precise cells responsible for PD duplications (Nacu et al., 2013). Similar to the effects of adding RA after the early/mid bud stage has commenced, *Rarβ* antagonism with the isoform-specific antagonist LE135 has no effect in early regeneration, but halts regeneration at the mid/late bud stage (Del Rincón and Scadding, 2002). Therefore, the differential effect of RA on developing and regenerating limbs might be due to its interactions with specific RARs during specific stages of regeneration or in specific cell types. RA's teratogenic capacity to truncate limbs rather than re-specify PD axis identity could be explained by dysregulation of specific RARs. It is fundamental to our understanding of limb development and regeneration to identify the molecular basis of proximodistal duplication versus truncation of the regenerating limb.

The cellular mechanisms that impart positional memory are still unclear (McCusker et al., 2015; Phan et al., 2015; Roensch et al., 2013). Several transcription factors have been identified that presumably activate genes responsible for positional memory (Crawford and Stocum, 1988), including *Meis1*, *Meis2* (Mercader et al., 2005), *Hoxd10* (Simon and Tabin, 1993) and *Hoxa13* (Gardiner et al., 1995), but our understanding of what makes a limb proximodistally duplicate, truncate, or grow the proper structure is lacking. Fundamental questions are unresolved including how many genes participate in PD positional memory, how these genes are coordinated at the cellular level, and whether salamander orphan genes regulate the positional memory required for regeneration. Thus, the objective of this study was to reveal the underlying basis of RA-induced PD duplications versus truncations utilizing transcriptomics, RARE-reporter animals, and RAR-specific agonists and antagonists.

RESULTS

Effects of RAR perturbation on limb development and regeneration

Our previous work showed that RAR reporter activity is present in regenerating limbs with expression mainly in epidermal keratinocytes, axons and nerve-associated cells. RA-induced PD duplication coincided with upregulation of RA reporter activity in connective tissue fibroblasts (Monaghan and Maden, 2012b). Here, we investigated whether endogenous RAR activity is required for limb regeneration. We treated regenerating animals with the selective RARβ antagonist LE135 (Li et al., 1999), because it has been shown to cause limb truncations and hypomorphic regenerates whereas RARα-specific and pan-RAR antagonists have minimal effects (Del Rincón and Scadding, 2002). At 7 days post amputation (dpa), RARβ antagonism induced reporter activity in RARE-EGFP limbs to a similar extent as RA-treated limbs, rather than decreasing activity as would be expected [Fig. 1A-C; n=6, ∼4 cm total length (TL)]. Reporter activity was mainly present within skeletal tissue including the perichondrium, in a few fibroblast-like cells, and within the basal wound epidermis compared with basal wound epidermis and fibroblasts in RA-treated limbs (Fig. 1C). Overall, RARE reporter activity had similar patterns of expression as RA-treated limbs except that LE135 induced RARE-EGFP more strongly in skeletal tissue.

RARβ antagonism did not halt blastema formation or initial growth. Rather, LE135 significantly halted growth at the mid bud blastema stage (Fig. 1D-F′), which corresponds approximately to the beginning of re-differentiation. After 15 days of treatment with a different RARβ antagonist, LE540 (Li et al., 1999), blastema size was 1.044±0.16 s.d. (n=5 right limbs) versus 1.312±0.12 s.d. in untreated limbs (n=6 right limbs) (Student's t-test, two-tailed; P=0.01) and had progressed to pallet stage compared with early digit formation in untreated limbs. Based upon these observations, we reasoned that RARβ inhibition might negatively impact endochondral ossification. Alcian Blue staining showed that some cartilaginous precursors (chondroblasts) are formed in LE135-treated limbs (Fig. 1E′ versus1F′) along with the expression of Collagen 2a protein (Fig. 1G versus 1H), but LE135-treated limbs showed a lack of progression from chondroblasts to chondrocytes as indicated by the formation of lacunae-like structures as shown in Fig. 1G (arrowheads) versus Fig. 1H.

We next tested whether RARβ antagonism also inhibits limb development through an RA-responsive transcriptional pathway. We found that RARβ antagonism, initiated at the onset of forelimb bud outgrowth (stage 36), slowed forelimb growth by the mid bud stage 43 (Fig. 1I) and growth ceased by stage 50 (Fig. 1J,K). RA reporter activity is known to be present in developing forelimbs, but is absent in developing hindlimbs (Monaghan and Maden, 2012b). We found that RARβ antagonism initiated at the onset of hindlimb bud outgrowth (stage 51) activated RARE-reporter activity 6 days later (Fig. 1L), and this corresponded with inhibition of hindlimb outgrowth (Fig. 1M). Reporter activity was increased in the epidermis and proximal mesenchyme, which is the region of chondrocyte differentiation in the developing limb (Fig. 1L). This shows that despite RA signaling having different *in vivo* patterns between forelimb and hindlimb development, RARβ antagonism generates a similar outcome. Several mechanisms might explain the induction of RARE activity after RARβ antagonism. One possibility is that LE135 is acting as an RARβ agonist instead of antagonist. A second possibility is that RARβ has an inhibitory role in the absence of ligand, normally preventing transcription of target genes, but when this inhibitory activity is inactivated, gene expression of RA target genes is induced. A similar inhibitory role of RARs occurs during mammalian chondrogenesis, when adding RAR antagonists induces gene expression of some RAR target genes (Weston et al., 2002, 2003b). Therefore, it is possible that transcriptional inhibition was removed with RARβ antagonism, inducing RARE-dependent gene expression programs.

Gene transcriptional responses to RAR perturbation

To test whether RARβ antagonism induces RARE-dependent transcriptional changes as well as delineate the molecular basis of RA-induced PD duplication versus truncation, we performed microarray gene expression analysis on forelimbs that will eventually regenerate normally (DMSO treated), become PD duplicated (RA treated) or become truncated (LE135 treated; Fig. 2A). Genes were identified as statistically significant if they had a false discovery rate (FDR)<0.05 determined by an ANOVA analysis (533 significant probe sets), and exhibited a >1.5-fold change (FC) relative to control DMSO samples in either treatment group (327 significantly changed probe sets). Surprisingly, high similarity was observed in gene expression between LE135- and RA-treated forelimbs despite yielding different phenotypes (Pearson's correlation coefficient between treatment groups using log2 fold change from DMSO=0.883). Pairwise comparisons between groups (FC>1.5 and FDR<0.05) showed that most genes

Development (2017) 144, 601-611 doi:10.1242/dev.139873

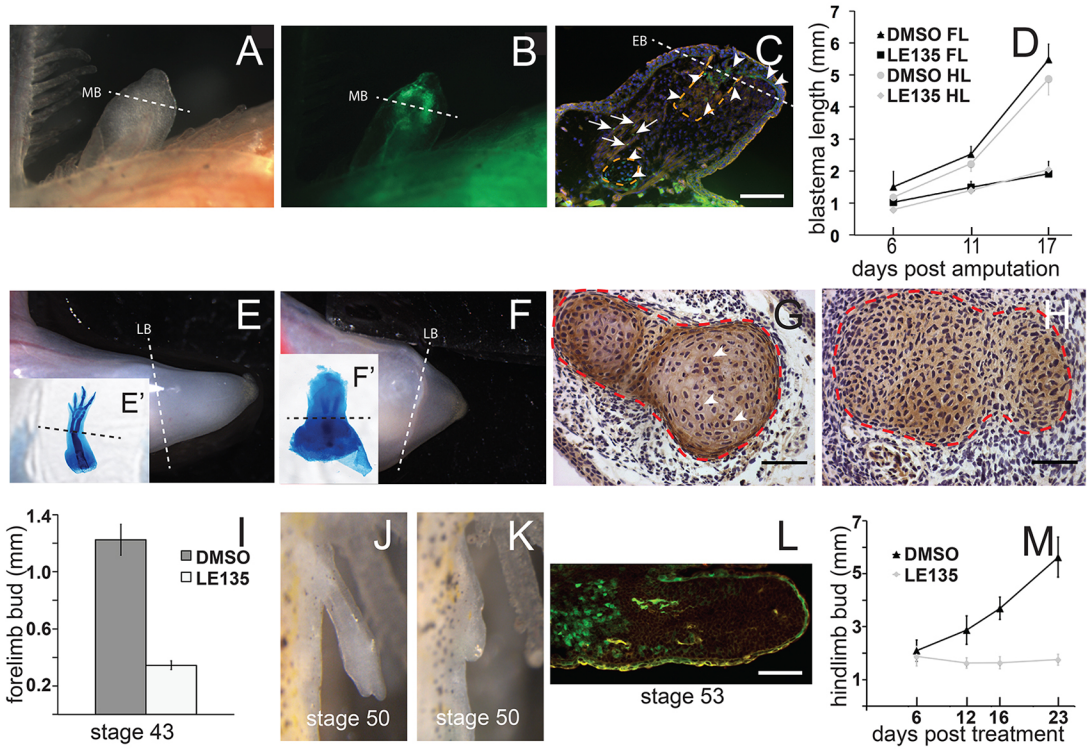

Fig. 1. Effect of LE135 on regenerating and developing limbs. (A,B) Example of LE135-treated RARE-EGFP forelimb amputated at the proximal zeugopod, collected at 6 dpa (2.3 cm SVL/4 cm TL). (C) Histological section of early bud limb amputated at the distal stylopod and treated with LE135 for 6 days. RARE-EGFP^{+} cells in skeleton and epidermis are indicated with arrowheads. Arrows indicate fibroblast-like cells in muscle. Orange dashed lines indicate skeletal elements. (D) Growth of DMSO- and LE135-treated regenerating forelimbs (FL) and hindlimbs (HL) after proximal zeugopod amputation at 6, 11 and 17 dpa (n=4 right limbs/group). Two-way ANOVA; $F(1,18)=141.44$, $P<0.001$ for treatment effect. (E,E′) Representative DMSO-treated forelimb at 11 dpa (3.9 cm SVL/7.0 cm TL) (stained with Alcian Blue in E′ after completion of limb regeneration). (F,F′) LE135-treated forelimb at 11 dpa (3.7 cm SVL, 6.3 cm TL) (stained with Alcian Blue in F′ after completion of regeneration). (G) Cross-section through regenerated zeugopod immunostained for Coll2a at 17 dpa. White arrowheads indicate chondrocytes in lucanae-like structures and red dashed line encircles radius/ulna. (H) LE135-treated regenerated forelimb sectioned through the zeugopod and immunostained for Coll2a at 17 dpa. (I) Size of developing forelimb at developmental stage 43 (n=4 DMSO right limbs, n=10 right LE135 limbs). Student's t-test, two-tailed; $P<0.001$. (J,K) DMSO-treated (J) and LE135-treated (K) developing limb with LE135 treatment stopping at stage 43 and images taken at stage 50. (L) Representative section of RARE-EGFP hindlimb at stage 53 after 6 days of LE135 treatment. (M) Growth of DMSO- (n=13 right limbs) and LE135-treated hindlimbs (n=10 right limbs) at 6, 12, 16 and 23 days post treatment starting at hindlimb bud initiation at stage 51. Two-way ANOVA; $F(1,87)=415.45$, $P<0.001$ for treatment effect. Error bars represent s.d. Dashed lines mark amputation plane. EB, early bud; LB, late bud; MB, mid bud. Scale bars: 250 µm (C,L); 200 µm (G,H).

upregulated after RA treatment were also upregulated after LE135 treatment (Fig. 2B) suggesting a similar transcriptional 'activating' response in both treatment groups. Many more genes were uniquely downregulated between RA- and LE135-treated groups suggesting a more divergent transcriptional 'silencing' response between PD duplication and truncation (Fig. 2C).

To classify quantitative differences between treatments, hierarchical clustering of significant genes was performed on all 327 significantly changed genes, which generated five distinct clusters (Fig. 2D). Cluster 1 (n=97) were on average upregulated after both treatments compared with controls. Cluster 2 (n=67) included genes that were on average higher in RA-treated samples. Cluster 3 (n=34) included genes that on average were unchanged in LE135-treated samples, but were upregulated after RA treatment (Table S1). In contrast, cluster 4 (n=14) contained genes that on average changed little after RARβ antagonism, but were downregulated during RA-induced PD duplication (Table S1). Lastly, cluster 5 (n=115) contained genes that were on average downregulated in both treatment groups. Overall, hierarchical clustering highlighted the dynamic transcriptional response that occurs after perturbation of RAR signaling.

We will first focus on common gene expression changes observed after either treatment. The most strikingly upregulated genes in both treatment groups were involved in the retinoic metabolic process (over-representation analysis) including genes involved in RA synthesis, shuttling to the nucleus, catabolism, and RA-dependent transcriptional activation and repression (Fig. 2E). This suggests that RA signaling increases in both treatment groups, even though RA was not introduced to LE135-treated limbs. One explanation for this is the upregulation of RA synthesis genes after LE135 treatment (Fig. 2E). Another group of commonly upregulated genes were involved in sterol metabolism including *Cyb5a*, *Soat1*, *Sdr16c5*, *Dhrs3*, *Gmds* and *Cyp4b1*. Other striking expression patterns in cluster 1 included the upregulation of genes associated with extracellular matrix production and breakdown including *Aggrecan*, *Brevican*, *Efemp1*, *Elfn1* and *Mmp13* as well as intracellular intermediate filaments including *Krt8*, *Krt15* and *Krt19*. It is clear that some common cellular changes are occurring in both PD duplicated and truncated limbs.

Gene transcriptional responses associated with RA-induced proximodistal duplications

We reasoned that identifying genes specifically induced or silenced during PD duplication compared with controls would reveal the underlying mechanism of RA-induced PD duplication. Therefore, we focused on clusters 2-4, which included differentially regulated genes

Development (2017) 144, 601-611 doi:10.1242/dev.139873

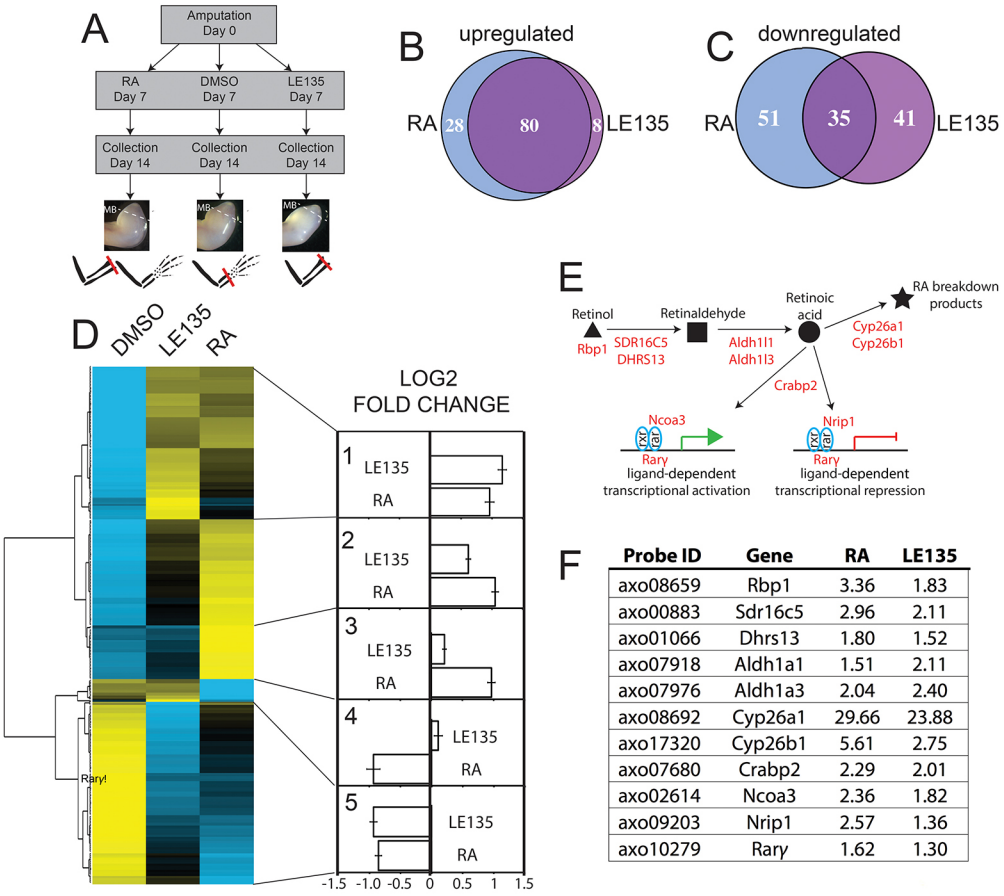

F

Probe ID	Gene	RA	LE135
axo08659	Rbp1	3.36	1.83
axo00883	Sdr16c5	2.96	2.11
axo01066	Dhrs13	1.80	1.52
axo07918	Aldh1a1	1.51	2.11
axo07976	Aldh1a3	2.04	2.40
axo08692	Cyp26a1	29.66	23.88
axo17320	Cyp26b1	5.61	2.75
axo07680	Crabp2	2.29	2.01
axo02614	Ncoa3	2.36	1.82
axo09203	Nrip1	2.57	1.36
axo10279	Rary	1.62	1.30

G

Gene	RA	LE135
Cyp26a1	18.69	12.86
Cyp26b1	3.60	1.57
Aldh1a1	0.94	1.18
Rarα	0.92	0.66
Rarβ	1.04	0.77
Rarγ	3.77	1.22

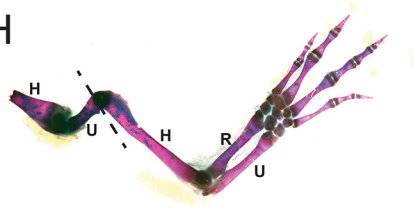

Fig. 2. Microarray analysis of regenerating limbs. (A) Schematic of microarray experimental design. Representative limbs from each treatment group are presented as well as the eventual outcomes of the experiment after the completion of regeneration. Red lines indicate the amputation plane of each treatment group. (B,C) Upregulated (B) and downregulated (C) genes from pairwise comparisons between RA/DMSO and LE135/DMSO.
(D) Heatmap displaying hierarchical clustering of 327 significantly changed genes. Five clusters show average log2 expression values ±s.e.m. for genes in each cluster. (E) Schematic of the RA metabolic and signaling pathway, highlighting (in red) genes upregulated after RA and LE135 treatment at each step of the RA signaling pathway.
(F) Table highlighting the expression patterns of the RA signaling genes highlighted in E. (G) qPCR validation of RA pathway genes. (H) PD duplication of a limb treated with the RARγ agonist CD1530 and stained with Alcian Blue and Alizarin Red. The amputation was performed at the distal zeugopod and the radius was lost or regressed. H, humerus; R, radius; U, ulna.

in RA-treated limbs compared with LE135-treated and DMSO-treated limbs. Although LE135 may have upregulated some of the same genes, clusters 2 and 3 show that the level of upregulation is on average much lower than RA-treated limbs. This might be due to the fact that many RA synthesis genes are upregulated after LE135 treatment. Many cluster 2/3 genes (n=101) are expressed in proximal developing limb buds in other limbed vertebrates or required for proper limb development [cluster 2 expressed in proximal limb: *Meis1* (Mercader et al., 2000, 2005), *Meis2* (Mercader et al., 2000, 2005), *Pbx1* (Selleri et al., 2001), *Arid5b* (Ristevski et al., 2001); cluster 2 expressed in limb bud: *Mia3* (Bosserhoff et al., 2004), *Rac1* (Bell et al., 2004; Suzuki et al., 2013), *Asph* (Patel et al., 2014), *Neo1* (Hong et al., 2012), *Cyp26B1* (MacLean et al., 2001), *Flrt2* (Haines et al., 2006), *Rarγ* (Pennimpede et al., 2010), *Rbp1* (Gustafson et al., 1993), *KIAA1217* (Semba et al., 2006); cluster 3 (Table S1) expressed in proximal limb: *Fibin* (Taher et al., 2011; Wakahara et al., 2007), *Epha7* (Araujo et al., 1998), *Nrip1* (Smith et al., 2014), *Rnd3* (Bell et al., 2004); cluster 3 expressed in limb bud: *Apcdd1* (Jukkola et al., 2004), *Zfn638* (Bell et al., 2004), *Stat3* (Gray et al., 2004), *Tsh2* (Caubit et al., 2000; Erkner et al., 1999)]. The association of these genes with limb patterning in other vertebrates supports the idea that RA reprograms the distal cells to resemble a proximal limb cell fate. It also suggests that PD duplication entails at least 100 genes. Genes that have been previously identified as upregulated after RA treatment in regenerating salamander limbs were also identified in our study including *Meis1* and *Meis2* (Mercader et al., 2005; Simon and Tabin, 1993), genes that are accepted as determining proximal fates in vertebrate limbs (Mercader et al., 2000; Roselló-Díez et al., 2011) (*Meis1* FC=+1.99 RA, FC=+1.35 LE135; *Meis2* FC=+1.92 RA, FC=+1.52 LE135).

Cluster 4 included 14 downregulated genes in RA-treated limbs compared with LE135-treated and DMSO-treated limbs (Table S1). Alox5 was the only exception because it was exclusively upregulated in RARβ antagonized limbs (LE135 versus DMSO +1.55-fold; RA versus DMSO −1.17). Seven of the 13 genes downregulated in RA-treated limbs are known to be expressed in the distal portion of the developing or regenerating vertebrate limb including *Lhx9* (Gu and Kania, 2010; Tzchori et al., 2009), *Zic5* (Merzdorf, 2007), *Lmo1* (Taher et al., 2011), *Lhx2* (Taher et al., 2011; Tzchori et al., 2009), *Spry1* (Minowada et al., 1999; Wang and Beck, 2014), *Msx2* (Bell et al., 2003; Carlson et al., 1998; Tribioli et al., 2002), *HoxA13* (Gardiner et al., 1995; Haack and Gruss, 1993; Scotti et al., 2015), most of which are required for distal identity in developing mouse limbs. This suggests that

Development (2017) 144, 601-611 doi:10.1242/dev.139873

distal-identity genes are silenced only in limbs undergoing PD duplication, similar to the transcriptional activation of proximal-identity genes during PD duplication.

Positional information is thought to reside on the cell surface of blastema cells (Stocum and Cameron, 2011) or in the extracellular matrix (Phan et al., 2015), which is supported by the fact that proximal blastemas engulf distal blastemas *in vitro* (Nardi and Stocum, 1984). Our data provide several candidate molecules for regulating positional information in clusters 2, 3 and 4 (n=115), which included 23 extracellular molecules (GO term: Extracellular Region) as well as 11 genes involved in the regulation of cell adhesion (GO term: Cell Adhesion). Overall, microarray analysis supports the idea that PD duplication entails both loss of distal cell identity and gain of proximal cell identity, and modifications in cell-cell contact and cell adhesion properties.

Rarγ in particular has been associated with regulating PD limb duplications (Pecorino et al., 1996). Our results show that RA-induced PD duplication increased *Rarγ* expression to 1.62-fold higher than controls (cluster 3) versus 1.30-fold in LE135-treated limbs. qPCR supports this finding and shows that RARα and RARβ are not upregulated in either treatment group (Fig. 2G). Previous work has shown that activation of RARδ alone, which is homologous to human RARγ, was able to proximalize cells whereas RARα and RARβ were incapable (Pecorino et al., 1996). To test whether activation of RARγ is also capable of proximalizing entire limb blastemas, we treated early blastemas with a potent RARγ selective agonist, CD1530. We find that RARγ agonist treatment of early limb blastemas was capable of mimicking RA treatment by generating PD duplications to the shoulder level (n=2; Fig. 2H). This result supports the hypothesis that RARγ is the key RAR regulating the PD limb axis during limb regeneration, although a more thorough analysis of other RAR agonists and antagonists is clearly needed to support this claim.

Gene transcriptional responses associated with limb truncations

RARβ antagonism inhibited limb growth leading to limb truncation during development and regeneration. Genes associated with limb truncation were found mainly in cluster 1 (Table S1). The first striking feature of cluster 1 is that it contains genes involved in skeletal formation and remodeling including the osteoblast master regulator gene *Sp7*, which is higher after RARβ antagonism (FC=+1.77 after LE135 treatment versus FC=+1.07 after RA treatment). Other genes known to be upregulated after osteoclastogenesis included *tank* (Maruyama et al., 2012) (FC=+1.51 after LE135 treatment), and lipid mediators including *Alox5* (cluster 5), *Alox15b* and *Aloxe3*. In mammals, loss of lipid mediators Alox5 and Alox15b leads to an increase in bone, and increase of the activity of these lipid mediators decreases bone density (O'Connor et al., 2014). Other gene expression patterns were suggestive for an effect on skeletal progenitor differentiation including a FC of +2.2 of *Tgfβ2* in LE135-treated limbs (FC=+1.73 in RA treated), a FC of +1.47 of *Tgfβ1* in LE135-treated limbs (FC=+3.30 in RA treated), and a significant downregulation of *Bmpr1b* (FC=−2.57 in LE135 and FC=−1.77 in RA-treated limbs). Although most differences between RARβ antagonism and RA-induced PD duplication were quantitative in nature, it seems that gene expression patterns were skewed towards a transcriptional program leading to skeletal regression.

RARβ antagonism induces a loss of long bone integrity

Considering the lack of skeletal differentiation that occurs in regenerating limbs after RARβ antagonism, we next investigated whether RARβ antagonism has an impact on uninjured bone integrity. RARβ antagonism led to a permanent shrunken limb phenotype (Fig. 3A-C). After 21 days of treatment in smaller animals, severe shrinking occurred [n=8 controls, snout to vent length (SVL)=2.5, TL=4.8, control stylopod+autopod=5.33±0.58 s.d., treated stylopod+autopod=2.49±0.82 s.d.; Student's t-test, two-tailed; P<0.001]. Integrity of long bones was strikingly impacted compared with untreated limbs, which was associated with an increase in RARE-EGFP reporter activity in long bones, epidermis and nerve axons (Fig. 3D), suggesting that the effect of LE135 could be partially cell intrinsic. Effects of RARβ antagonism included a compaction of the metaphysis and diaphysis with little effect on the epiphysis and an increase in osteoclasts within the diaphysis of bones (Fig. 3F,G). Defects were clearly apparent after microCT evaluation at 12 days of treatment, although no significant decrease in radius/ulna length could be observed at this point. Overall, the loss of bone homeostasis is consistent with gene expression profiles described in the results section above. Animals had an excess amount of skin, suggesting that degeneration was specific to the skeleton (Fig. 3H versus 3I). Furthermore, the cartilaginous epiphysis of treated limbs and carpals of the hands were of normal size (Fig. 3A versus 3B) suggesting degeneration of differentiated chondrocytes. Overall, long bone degeneration caused by RARβ antagonism seems to be due to an active transcriptional response within the differentiating skeletal cells, which is associated with significant osteoclastogenesis.

RARβ antagonism negatively impacts vertebral growth and epimorphic tail regeneration

We next investigated whether the negative impact of RAR perturbation was specific to the limb. LE135 treatment for 21 days resulted in scoliosis of the spine demonstrating that the effects of RARβ antagonism also occurred in other skeletal tissues (Fig. 4A-C). RARE-EGFP animals show that RA reporter activity is minimal in the uninjured spinal column, except in spinal cord axons and a few cartilage cells (Fig. 4D). Upon RARβ antagonism, reporter activity increased in chondrocytes surrounding the spinal cord, especially in the dorsal chondrification center of the neural arch (Fig. 4E). In contrast, RA treatment induced reporter activity primarily in neural progenitor cells of the spinal cord, some white matter cells, the neural meninges, and cells resembling fibroblasts in the muscle (Fig. 4F). Altogether, these data strongly suggest that RARβ antagonism induces a specific RA-transcriptional response in skeletal tissue, which leads to a loss of skeletal integrity, possibly through a loss of homeostatic regenerative ability. RA induces a more specific response in fibroblastic cells, supporting the idea that RA specifically reprograms fibroblast cell identity.

Based upon the similar RAR-dependent reporter activity in uninjured tails and limbs, we next assessed whether RARβ antagonism also impacts tail regeneration. Indeed, RA reporter activity was primarily localized in axons of the untreated regenerating spinal cord (Fig. 4G-I), whereas RARβ antagonism induced significant reporter activity in differentiating prechondrocytes and epidermis (Fig. 4J-L). RA treatment increased reporter activity in spinal cord neural progenitor cells and some fibroblasts (Fig. 4M-O), which could explain the inhibitory properties of RA on spinal cord cell proliferation and urodele tail regeneration (Pietsch, 1993). RA is also known to regulate neural differentiation across vertebrates (Maden, 2007). The similar responses of RA treatment and RARβ antagonism between the limb and tail suggests that there may be a common RAR gene expression program regulating both limb and tail regeneration. Overall, the contrasting cell types

Development (2017) 144, 601-611 doi:10.1242/dev.139873

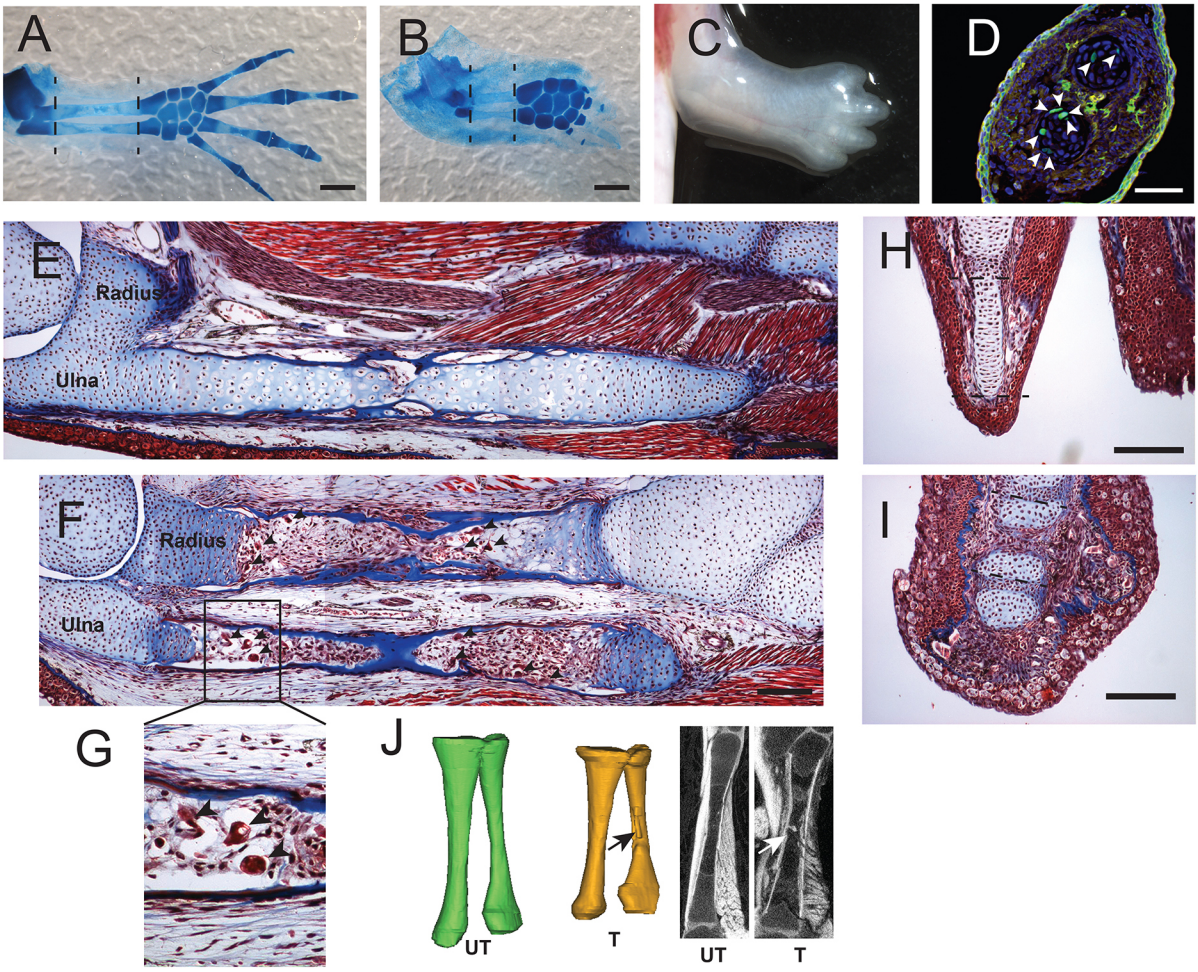

Fig. 3. Effect of LE135 treatment in developed limbs. (A) Example of DMSO control limb stained with Alcian Blue (SVL=5.9 cm, TL=10 cm). Dashed line indicates diaphysis. (B) Uninjured limb treated with LE135 for 21 days. (C) Unstained LE135-treated uninjured limb. (D) RARE-EGFP uninjured zeugopod treated with LE135 for 6 days. Arrowheads indicate RARE-EGFP^{+} cells in radius/ulna. (E,F) Masson's trichome staining of uninjured zeugopod untreated (E) or treated with LE135 for 14 days (F). Red stain shows muscle, epidermis, nerve and blood/inflammatory cells. Blue stain highlights bone and cartilage. Black stains nuclei. Osteoclasts are indicated with arrowheads. (G) Close-up of degenerating ulna with osteoclasts indicated by arrowheads. (H) Uninjured digit. Dashed lines indicate distal phalange. (I) LE135-treated digit. Dashed lines indicate shrunken intermediate phalange. (J) µCT 3D rendering of untreated limbs (UT) and limbs treated with LE135 for 12 days (T) and cross-sections of untreated and treated limbs with defects in treated limbs indicated by the arrow. Scale bars: 1 mm (A,B); 250 µm (D-I).

responding to RA treatment versus RARβ antagonism also suggests that the role of RARs during regeneration is partially cell type dependent.

DISCUSSION

In this study, we show that modulation of RAR activity has a significant impact on tissue patterning and differentiation during epimorphic regeneration and skeletal homeostasis. We utilized reporter animals and gene microarrays to show that pharmacological activation of RARs with RA treatment, presumably through RARγ activation (Fig. 2G), induced a proximalization program leading to limb PD duplications. RARβ antagonism negatively affected skeletal differentiation and growth during epimorphic limb and tail regeneration and induced a skeletal regression program in uninjured skeleton. RARE-EGFP animals showed that induction of each transcriptional program had some overlap between tissue types, but also showed unique expression patterns – chondrocytes in the case of the truncation program and fibroblasts in the case of the PD duplication program (Fig. 4P). We propose that proper RAR activation is essential in a cell type-dependent and temporal manner. Overall, highly regulated RAR activity controls crucial transcriptional networks required for tissue patterning, differentiation, and tissue turnover during both epimorphic regeneration and homeostasis.

The endogenous role of RARs during tissue regeneration is unclear. We show that an RARγ agonist alone is sufficient for PD limb duplications, suggesting that RARγ might regulate patterning. This is supported by a microarray study (Voss et al., 2015) showing that *Rarγ* transcripts increase at the onset of blastema formation and stabilize thereafter. qPCR analysis also shows that only RARγ, not RARα or RARβ, is upregulated during PD duplication (Fig. 2G). These results together reinforce findings that RARγ is capable of proximalizing distal newt blastema cells, but RARα and RARβ cannot (Pecorino et al., 1996), and the fact that RARα antagonists have little impact on axolotl limb regeneration (Del Rincón and Scadding, 2002). It is possible that RARγ activity sets the appropriate PD level of the early blastema and overactivation with agonists sets the level to a proximal fate.

Few studies have screened for genes involved in positional re-specification of the limb. One exception used subtractive cDNA screening to identify upregulated and downregulated genes in distal newt blastemas after RA treatment (da Silva et al., 2002). This study identified one salamander-specific molecule (Geng et al., 2015),

Development (2017) 144, 601-611 doi:10.1242/dev.139873

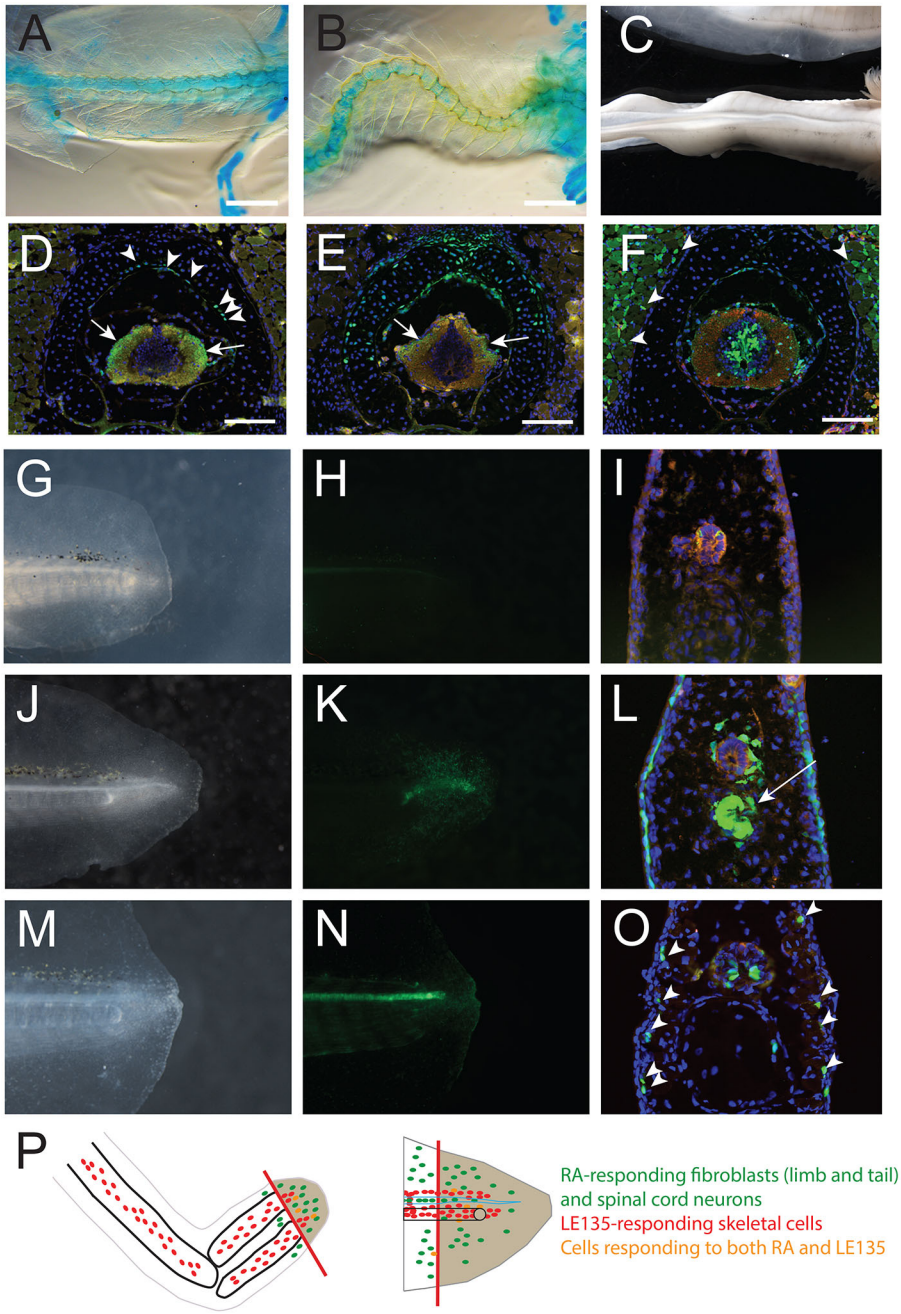

Fig. 4. Effect of LE135 treatment in developed and regenerating tails. (A) Uninjured spinal column of 5.2 cm TL animal stained with Alcian Blue. (B) Spinal column of an animal treated with LE135 for 21 days. (C) Scoliosis in an LE135-treated animal. (D-F) Cross-section of uninjured (D), LE135-treated (E) and RA-treated (F) RARE-EGFP animals (SVL=3.5 cm; TL=6 cm). Arrows in D,E indicate spinal cord RARE-EGFP+ axons; arrowheads in D indicate perichondrium of vertebrae. Arrowheads in F indicate fibroblast-like cells around muscle. (G-O) Live images and cross-sections from regenerating tails of ~4 cm TL RARE-EGFP axolotls 7 dpa without treatment (G-I), after LE135 treatment for 5 days (arrow indicates differentiating cartilage tube) (J-L) or after RA treatment for 5 days (arrowheads indicate fibroblast-like cells) (M-O). (P) Schematic showing a regenerating arm and regenerating tail proposing a model of cell responses to RA and LE135. The tan areas represent the regeneration blastema. Green cells represent the populations most commonly responding to RA treatment. Red cells primarily respond to LE135, whereas orange cells are responding to both RA and LE135. Scale bars: 2 mm (A,B); 250 µm (D-F).

prod1, that has a PD gradient in newts and can proximalize distal blastemal cells in newts and axolotls (Echeverri and Tanaka, 2005). We did not observe an upregulation of axolotl *Prod1* after RA treatment, which supports the finding that *Prod1* transcripts are more abundant in distal blastemas compared with proximal blastemas in axolotls (McCusker et al., 2015). The current model is that Prod1 signals through epidermal growth factor receptor to induce *Mmp9* expression (Blassberg et al., 2011). In our study, *Mmp9* was not differentially regulated between treatment groups although it is upregulated during the early stages of limb regeneration (Monaghan et al., 2009; Yang et al., 1999). Considering that Prod1 is predicted to be a secreted molecule in all other salamanders (Blassberg et al., 2011), it will be important to test whether it plays an endogenous functional role in the axolotl and is required for PD limb patterning as it is in newts (Kumar et al., 2015).

One model for vertebrate limb patterning is that trunk-derived mesoderm generates a proximal source of RA, which induces expression of the stylopod-specific homeobox genes *Meis1* and *Meis2* (Cooper et al., 2011; Rosello-Diez et al., 2014; Roselló-Díez et al., 2011). RA signaling is inhibited distally by Fgfs (Cooper et al., 2011; Mariani et al., 2008) and Cyp26b (Yashiro et al., 2004), which is supported by genetic ablation of distal Fgf genes (Mariani et al., 2008) or *Cyp26b* (Yashiro et al., 2004). Our data partially support this model as we observed clear upregulation of proximal *Meis1* and *Meis2* genes and the downregulation of *Sprouty1*, a gene upregulated by FGF signaling after RA treatment (Minowada et al., 1999; Wang and Beck, 2014). Furthermore, clusters 2-4 clearly showed an induction of proximally expressed genes and silencing of distally expressed genes. The permanent change in PD cell identity is likely to require restructuring of the epigenetic landscape. In

Development (2017) 144, 601-611 doi:10.1242/dev.139873

support of this hypothesis, we found that *Ncoa3*, the key ligand-dependent co-activator of RAR target genes (Torchia et al., 1997), was upregulated during PD duplication (Fig. 2E,F). Furthermore, *Nrip1*, the key ligand-dependent co-repressor of RAR target genes (Hu et al., 2004) was also upregulated (Fig. 2E,F) as well as the downregulation of the histone methyltransferase *Whsc1* (Nimura et al., 2009) and differential expression of many homeobox-containing genes (*Meis1*, *Meis2*, *Pbx1*, *Hoxc5*, *Tshz2*, *Zhx1*, *Zfhx4*, *Msx2*, *Hoxa13*, *Lhx2*, *Dlx6* and *Lhx9*). Together, this group of genes is likely to be crucial for re-specification of positional information in the regenerating limb.

The similarity in gene expression between PD duplication and truncation (Fig. 2) was surprising considering the divergent phenotypes. For example, genes associated with the proximal identity of vertebrate limbs, including *Meis1*, *Meis2* and *Pbx1*, were upregulated in both treatment groups. This may be explained by the fact that RA synthesis genes are upregulated after LE135 treatment and *Meis* expression is due to new RA synthesis. Alternatively, it could be accounted for by the fact that Meis proteins are expressed after axolotl limb amputation in muscle blastema cells (Nacu et al., 2013) and epithelium (Nacu et al., 2016), which probably respond differently than fibroblast-expressing Meis. Another possible scenario is that RARβ antagonism might partially reprogram PD identity, but the program is incomplete or the truncation transcriptional program overrides the PD program. Regardless, genes found in cluster 3 including *Tshz2*, *Tll2*, *Htra3*, *Fibin* and *Cetp* might be new indicators of limb proximalization, supplementing classical indicators of proximal limb identity. A limitation of our study is that whole blastemas were analyzed rather than fibroblasts specifically. It would be interesting in the future to assess global gene expression changes only in fibroblasts, which are the cells known to regulate positional information of the limb.

Our data suggest that the mechanism by which LE135 inhibits epimorphic regeneration is through disruption of endochondral ossification. This leads to the question of how an antagonist can increase RAR target gene expression. During chondrogenesis, RARs play a repressive function; ligand-less RARs/RXRs recruit repressive transcriptional complexes to RA target gene promoters, which allow the chondrogenesis program to progress. *In vitro*, RAR-mediated repression is required for chondrocyte differentiation (Weston et al., 2003a, 2002). Chondrogenesis is also inhibited by agonists for RARα (Shimono et al., 2010; Weston et al., 2002) or RARγ (Shimono et al., 2011; Williams et al., 2009) (promotes RAR transcriptional activity) and enhanced by RAR reverse agonists (Williams et al., 2009) (promotes RAR transcriptional repression). In *Cyp26b1* null mice (excess RA), skeletal prechondrocytes begin to differentiate, but exhibit reduced chondrocyte differentiation (Dranse et al., 2011). In our study, a similar mechanism might occur in that LE135 inhibits the repressive function of RARβ, activating the wrong transcriptional program in prechondrocytes (cluster 1 and Alox5). This could account for the similar gene expression patterns observed between RA treatment and LE135 treatment.

In vertebrates, long bones undergo continuous turnover, otherwise known as homeostatic regeneration, through osteoblast-based addition and osteoclast resorption. Excessive RA signaling is known to impact homeostatic turnover and skeletal integrity of long bones, including conditions like hypervitaminosis A (Green et al., 2016; Henning et al., 2015). Excess RA signaling increases osteoclast formation in mammals *in vitro* and *in vivo* (Henning et al., 2015); this is also observed in our studies after LE135 treatment i.e. increased RA reporter activity in skeletal tissue (Fig. 3D and Fig. 4P), increased osteoclastic gene expression, and increased numbers of osteoclasts in resorbing bone (Fig. 3F,G). Furthermore, *in vivo* data suggest that loss of RAR repression leads to accelerated chondrocyte hypertrophy (Dranse et al., 2011), which we also observed after LE135 treatment (Fig. 3F). It is likely that in our studies, increased RA signaling is context dependent – RA ligand-based RA signaling might not shrink skeletal tissue, but LE135-induced transcription does promote resorption. The transcriptional responses specific to LE135 treatments should provide insight into RA signaling-induced bone resorption.

Our study further elucidates the roles of RARs during regeneration, but also brings to light several unknowns about limb regeneration. The most pressing of which is whether endogenous RA ligands are required for limb regeneration and whether the PD duplication of the limb is exclusively regulated by RARγ. Furthermore, it will be important to determine the functions of genes regulated by RARs during PD duplication; are they capable of determining proximodistal identity and are they required for the process? The results presented here provide crucial information for tackling these problems.

MATERIALS AND METHODS

Animal procedures

Ambystoma mexicanum (axolotls) were bred in captivity either at the University of Florida or Northeastern University. Experiments were performed in accordance with University of Florida and Northeastern University Institutional Animal Care and Use Committees. For all experiments, animals were anesthetized by treatment of 0.01% benzocaine. In all cases of amputations, the radius/ulna or femur were trimmed to make a flush amputation plane and limb staging was performed according to Armstrong and Malacinski (1989) and Nye et al. (2003). Animals were bathed in drug [RA, 1 µM (Sigma); LE135 (Tocris), 250 nM; CD1530 (Tocris), 250 nM; LE540 (Wako), 1 µM; 0.03% DMSO (Sigma)] for the designated times with water changes every other day or every day for the microarray experiment.

Histology and immunohistochemistry

RARE-EGFP sections were fixed in 4% paraformaldehyde at 4°C overnight, cryomounted in OCT medium (TissueTek), sectioned at 15-20 µm, stained in Hoechst 33258, and mounted in 80% glycerol. Histology was performed by fixing tissues in 10% neutral buffered formalin at 4°C overnight, washing twice in PBS, processing for paraffin embedding, and sectioning at 8 µm. Masson's Trichrome staining was performed according to the manufacturer's protocol (Richard Allen).

Whole-mount skeletal staining

Limbs were fixed in 10% neutral buffered formalin overnight at 4°C and washed three times in PBS for 10 min. Limbs were then placed on a rocker overnight in 30% acetic acid/70% ethanol/0.3% Alcian Blue stain. When skeletal elements were visibly stained, they were treated with 0.1% trypsin in saturated sodium borate until clear. Some limbs were then treated with Alizarin Red in 1% KOH, then rehydrated in an ethanol series (100%, 95%, 70% and ddH_2O) and run through a 1% KOH/glycerol series of 3:1, 1:1, 1:3 and imaged using a Leica M165 FC stereomicroscope.

Microarray analysis

Juvenile axolotls 8.8 cm total length (TL) (high=10.1 cm, low=7.4 cm) and 4.58 cm average snout to vent length (SVL) received forelimb amputations at the distal zeugopod. Between days 7 and 14 dpa, individually housed animals were dosed with RA, LE135 or DMSO (n=16/treatment). Drugs were changed every other day. Blastemas containing as little stump tissue as possible were collected from all 48 animals at 14 dpa and single forelimbs from four separate individuals were pooled together to yield four independent biological replicate samples for each treatment group. Total RNA was extracted using the Qiagen RNeasy Kit following the manufacturer's instructions. RNA quality was assessed using an Epoch

Development (2017) 144, 601-611 doi:10.1242/dev.139873

microplate spectrophotometer, gel electrophoresis, and a 2100 Agilent Bioanalyzer. RNA samples were processed and hybridized to custom *A. mexicanum* (Amby_002) Affymetrix GeneChips (Huggins et al., 2012) at the University of Kentucky Microarray Core. Expression values were generated using the Robust Microarray Average (RMA) algorithm (Irizarry et al., 2003) and data analysis was performed using the limma software package (Ritchie et al., 2015) in the R environment, generating overall significance statistical values and pairwise comparisons between groups. Venn diagrams were generated using significance values generated for RA/DMSO and LE135/DMSO using the VennDiagram package (Chen and Boutros, 2011). Hierarchical clustering was performed on all 327 significantly changed genes using Cluster (de Hoon et al., 2004) after Log2 transforming the data and mean-centering. Pearson's correlation and average linkage were used to generate a similarity matrix. Trees were visualized using Java TreeView (Saldanha, 2004).

Quantitative real-time qPCR

Real-time quantitative PCR collection times were the same as the microarray and biological replicates included four RA-treated samples, four LE135-treated samples and three DMSO-treated controls. cDNA was generated using the Thermo Verso cDNA Synthesis Kit and qPCR with gene-specific primers was performed with ABI PowerSYBR Green PCR Master Mix on a Step-One Plus system following the manufacturer's recommendations. Primers used were: Cyp26a1_F GTGTACCCCGTGGACAATCT, Cyp26a1_R TGCTATGGGTGTTGGGTTTA; Cyp26b1_F CCCTGCTGTAATGGAAGGAT, Cyp26b1_R CGAAGGGCACAATAGGTTTT; Aldh1a1_F AAGACATCGACAAGGCACTG, Aldh1a1_R CCAAAAGGACACTGTGAGGA; Aldh1a2_F GCCAAGACGGTCACAATAAA; Aldh1a2_R CATTCCTGAGTGCTGTTGCT; RARA_F ATACTTGGCAGCCAGAAGGT, RARA_R GCCAACGTTGTATGCATCTC; RARB_F AAAACTCTGAGGGGCTTGAA, RARB_R CTGGTGTGGATTCTCCTGTG; RARG_F CTTCTGCGTTTGATCCTTCA, RARG_R AGTGAGTATGGGGCTGTTCC. Genes were normalized to the control gene FCGBP, which was selected as unchanged in the microarray experiment (primers: FCGBP_F GTTTATGTGGCAGCCTCTCA, FCGBP_R GCCAGCATTAGCTGTGATGT). ΔΔCt was used to calculate fold changes from DMSO controls using the average ΔCt value for each sample.

Microcomputed tomography

Treated and control forearms (n=4) were skinned, fixed for 24 h in 10% buffered formalin and then incubated for 24 h in 70% ethanol at room temperature. They were then stained in a 1% phosphotungstic acid/70% ethanol solution for 24 h. The limbs were scanned in the same solution using a microcomputed tomography system (μCT 35, Scanco Medical) (Doube et al., 2010). Scans were acquired with an isotropic resolution of 6 μm, an integration time of 400 ms and a power of 55 kVp. Using BoneJ, we determined the length and the cross-sectional area at midshaft for the radius and the ulna. We reconstructed 3D images of the radius and ulna with the software Mimics.

Acknowledgements

We thank the many undergraduate volunteers in the Monaghan lab for animal care and discussions about the study.

Competing interests

The authors declare no competing or financial interests.

Author contributions

M.N., P.S. and J.R.M. contributed to experimental design, experimentation, analysis of results and writing of the manuscript. J.P. and S.J.S contributed to experimentation. M.M. and S.R.V. contributed to experimental design, analysis of results and writing of the manuscript. All authors read and approved the manuscript.

Funding

This work was funded by Northeastern University (Start-up funds to J.R.M.), a National Science Foundation grant (1558017 to J.R.M. and M.M.), and the US Army Research Office (56157-LS-MUR to S.R.V.).

Data availability

Microarray data have been deposited in NCBI GEO under accession number GSE93303.

Supplementary information

Supplementary information available online at
http://dev.biologists.org/lookup/doi/10.1242/dev.139873.supplemental

References

Araujo, M., Piedra, M. E., Herrera, M. T., Ros, M. A. and Nieto, M. A. (1998). The expression and regulation of chick EphA7 suggests roles in limb patterning and innervation. *Development* **125**, 4195-4204.

Armstrong, J. B. and Malacinski, G. B. (1989). *Developmental Biology of the Axolotl*. New York: Oxford University Press.

Bell, S. M., Schreiner, C. M., Waclaw, R. R., Campbell, K., Potter, S. S. and Scott, W. J. (2003). Sp8 is crucial for limb outgrowth and neuropore closure. *Proc. Natl. Acad. Sci. USA* **100**, 12195-12200.

Bell, G. W., Yatskievych, T. A. and Antin, P. B. (2004). GEISHA, a whole-mount in situ hybridization gene expression screen in chicken embryos. *Dev. Dyn.* **229**, 677-687.

Blassberg, R. A., Garza-Garcia, A., Janmohamed, A., Gates, P. B. and Brockes, J. P. (2011). Functional convergence of signalling by GPI-anchored and anchorless forms of a salamander protein implicated in limb regeneration. *J. Cell Sci.* **124**, 47-56.

Blum, N. and Begemann, G. (2012). Retinoic acid signaling controls the formation, proliferation and survival of the blastema during adult zebrafish fin regeneration. *Development* **139**, 107-116.

Blum, N. and Begemann, G. (2013). The roles of endogenous retinoid signaling in organ and appendage regeneration. *Cell. Mol. Life Sci.* **70**, 3907-3927.

Bosserhoff, A. K., Moser, M. and Buettner, R. (2004). Characterization and expression pattern of the novel MIA homolog TANGO. *Gene Expr. Patterns* **4**, 473-479.

Carlson, M. R. J., Bryant, S. V. and Gardiner, D. M. (1998). Expression of Msx-2 during development, regeneration, and wound healing in axolotl limbs. *J. Exp. Zool.* **282**, 715-723.

Carter, C., Clark, A., Spencer, G. and Carlone, R. (2011). Cloning and expression of a retinoic acid receptor β2 subtype from the adult newt: evidence for an early role in tail and caudal spinal cord regeneration. *Dev. Dyn.* **240**, 2613-2625.

Caubit, X., Coré, N., Boned, A., Kerridge, S., Djabali, M. and Fasano, L. (2000). Vertebrate orthologues of the Drosophila region-specific patterning gene teashirt. *Mech. Dev.* **91**, 445-448.

Chambon, P. (1996). A decade of molecular biology of retinoic acid receptors. *FASEB J.* **10**, 940-954.

Chen, H. and Boutros, P. C. (2011). VennDiagram: a package for the generation of highly-customizable Venn and Euler diagrams in R. *BMC Bioinformatics* **12**, 35.

Clagett-Dame, M. and DeLuca, H. F. (2002). The role of vitamin A in mammalian reproduction and embryonic development. *Annu. Rev. Nutr.* **22**, 347-381.

Cooper, K. L., Hu, J. K.-H., ten Berge, D., Fernandez-Teran, M., Ros, M. A. and Tabin, C. J. (2011). Initiation of proximal-distal patterning in the vertebrate limb by signals and growth. *Science* **332**, 1083-1086.

Crawford, K. and Stocum, D. L. (1988). Retinoic acid coordinately proximalizes regenerate pattern and blastema differential affinity in axolotl limbs. *Development* **102**, 687-698.

Cuervo, R. and Chimal-Monroy, J. (2013). Chemical activation of RARbeta induces post-embryonically bilateral limb duplication during Xenopus limb regeneration. *Sci. Rep.* **3**, 1886.

da Silva, S. M., Gates, P. B. and Brockes, J. P. (2002). The newt ortholog of CD59 is implicated in proximodistal identity during amphibian limb regeneration. *Dev. Cell* **3**, 547-555.

de Hoon, M. J. L., Imoto, S., Nolan, J. and Miyano, S. (2004). Open source clustering software. *Bioinformatics* **20**, 1453-1454.

Del Rincón, S. V. and Scadding, S. R. (2002). Retinoid antagonists inhibit normal patterning during limb regeneration in the axolotl, Ambystoma mexicanum. *J. Exp. Zool.* **292**, 435-443.

Doube, M., Kłosowski, M. M., Arganda-Carreras, I., Cordelières, F. P., Dougherty, R. P., Jackson, J. S., Schmid, B., Hutchinson, J. R. and Shefelbine, S. J. (2010). BoneJ: free and extensible bone image analysis in ImageJ. *Bone* **47**, 1076-1079.

Dranse, H. J., Sampaio, A. V., Petkovich, M. and Underhill, T. M. (2011). Genetic deletion of Cyp26b1 negatively impacts limb skeletogenesis by inhibiting chondrogenesis. *J. Cell. Sci.* **124**, 2723-2734.

Duester, G. (2013). Retinoid signaling in control of progenitor cell differentiation during mouse development. *Semin. Cell Dev. Biol.* **24**, 694-700.

Echeverri, K. and Tanaka, E. M. (2005). Proximodistal patterning during limb regeneration. *Dev. Biol.* **279**, 391-401.

Erkner, A., Gallet, A., Angelats, C., Fasano, L. and Kerridge, S. (1999). The role of Teashirt in proximal leg development in Drosophila: ectopic Teashirt expression reveals different cell behaviours in ventral and dorsal domains. *Dev. Biol.* **215**, 221-232.

Gardiner, D. M., Blumberg, B., Komine, Y. and Bryant, S. V. (1995). Regulation of HoxA expression in developing and regenerating axolotl limbs. *Development* **121**, 1731-1741.

Geng, J., Gates, P. B., Kumar, A., Guenther, S., Garza-Garcia, A., Kuenne, C., Zhang, P., Looso, M. and Brockes, J. P. (2015). Identification of the orphan gene Prod 1 in basal and other salamander families. *Evodevo* **6**, 9.
Giguère, V., Ong, E. S., Evans, R. M. and Tabin, C. J. (1989). Spatial and temporal expression of the retinoic acid receptor in the regenerating amphibian limb. *Nature* **337**, 566-569.
Grandel, H., Lun, K., Rauch, G.-J., Rhinn, M., Piotrowski, T., Houart, C., Sordino, P., Küchler, A. M., Schulte-Merker, S., Geisler, R. et al. (2002). Retinoic acid signalling in the zebrafish embryo is necessary during pre-segmentation stages to pattern the anterior-posterior axis of the CNS and to induce a pectoral fin bud. *Development* **129**, 2851-2865.
Gray, P. A., Fu, H., Luo, P., Zhao, Q., Yu, J., Ferrari, A., Tenzen, T., Yuk, D. I., Tsung, E. F., Cai, Z. et al. (2004). Mouse brain organization revealed through direct genome-scale TF expression analysis. *Science* **306**, 2255-2257.
Green, A. C., Martin, T. J. and Purton, L. E. (2016). The role of vitamin A and retinoic acid receptor signaling in post-natal maintenance of bone. *J. Steroid Biochem. Mol. Biol.* **155**, 135-146.
Gu, W. X. W. and Kania, A. (2010). Identification of genes controlled by LMX1B in E13.5 mouse limbs. *Dev. Dyn.* **239**, 2246-2255.
Gustafson, A. L., Dencker, L. and Eriksson, U. (1993). Non-overlapping expression of CRBP I and CRABP I during pattern formation of limbs and craniofacial structures in the early mouse embryo. *Development* **117**, 451-460.
Haack, H. and Gruss, P. (1993). The establishment of murine Hox-1 expression domains during patterning of the limb. *Dev. Biol.* **157**, 410-422.
Haines, B. P., Wheldon, L. M., Summerbell, D., Heath, J. K. and Rigby, P. W. J. (2006). Regulated expression of FLRT genes implies a functional role in the regulation of FGF signalling during mouse development. *Dev. Biol.* **297**, 14-25.
Henning, P., Conaway, H. H. and Lerner, U. H. (2015). Retinoid receptors in bone and their role in bone remodeling. *Front. Endocrinol.* **6**, 31.
Hill, D. S., Ragsdale, C. W., Jr. and Brockes, J. P. (1993). Isoform-specific immunological detection of newt retinoic acid receptor delta 1 in normal and regenerating limbs. *Development* **117**, 937-945.
Hong, M., Schachter, K. A., Jiang, G. and Krauss, R. S. (2012). Neogenin regulates Sonic Hedgehog pathway activity during digit patterning. *Dev. Dyn.* **241**, 627-637.
Hu, X., Chen, Y., Farooqui, M., Thomas, M. C., Chiang, C.-M. and Wei, L.-N. (2004). Suppressive effect of receptor-interacting protein 140 on coregulator binding to retinoic acid receptor complexes, histone-modifying enzyme activity, and gene activation. *J. Biol. Chem.* **279**, 319-325.
Huggins, P., Johnson, C. K., Schoergendorfer, A., Putta, S., Bathke, A. C., Stromberg, A. J. and Voss, S. R. (2012). Identification of differentially expressed thyroid hormone responsive genes from the brain of the Mexican Axolotl (Ambystoma mexicanum). *Comp. Biochem. Physiol. C Toxicol. Pharmacol.* **155**, 128-135.
Irizarry, R. A., Hobbs, B., Collin, F., Beazer-Barclay, Y. D., Antonellis, K. J., Scherf, U. and Speed, T. P. (2003). Exploration, normalization, and summaries of high density oligonucleotide array probe level data. *Biostatistics* **4**, 249-264.
Jukkola, T., Sinjushina, N. and Partanen, J. (2004). Drapc1 expression during mouse embryonic development. *Gene Expr. Patterns* **4**, 755-762.
Kim, W.-S. and Stocum, D. L. (1986). Retinoic acid modifies positional memory in the anteroposterior axis of regenerating axolotl limbs. *Dev. Biol.* **114**, 170-179.
Knapp, D., Schulz, H., Rascon, C. A., Volkmer, M., Scholz, J., Nacu, E., Le, M., Novozhilov, S., Tazaki, A., Protze, S. et al. (2013). Comparative transcriptional profiling of the axolotl limb identifies a tripartite regeneration-specific gene program. *PLoS ONE* **8**, e61352.
Kragl, M., Knapp, D., Nacu, E., Khattak, S., Maden, M., Epperlein, H. H. and Tanaka, E. M. (2009). Cells keep a memory of their tissue origin during axolotl limb regeneration. *Nature* **460**, 60-65.
Kumar, A., Gates, P. B., Czarkwiani, A. and Brockes, J. P. (2015). An orphan gene is necessary for preaxial digit formation during salamander limb development. *Nat. Commun.* **6**, 8684.
Li, Y., Hashimoto, Y., Agadir, A., Kagechika, H. and Zhang, X.-K. (1999). Identification of a novel class of retinoic acid receptor beta-selective retinoid antagonists and their inhibitory effects on AP-1 activity and retinoic acid-induced apoptosis in human breast cancer cells. *J. Biol. Chem.* **274**, 15360-15366.
Lohnes, D., Mark, M., Mendelsohn, C., Dolle, P., Dierich, A., Gorry, P., Gansmuller, A. and Chambon, P. (1994). Function of the retinoic acid receptors (RARs) during development (I). Craniofacial and skeletal abnormalities in RAR double mutants. *Development* **120**, 2723-2748.
Ludolph, D. C., Cameron, J. A. and Stocum, D. L. (1990). The effect of retinoic acid on positional memory in the dorsoventral axis of regenerating axolotl limbs. *Dev. Biol.* **140**, 41-52.
MacLean, G., Abu-Abed, S., Dollé, P., Tahayato, A., Chambon, P. and Petkovich, M. (2001). Cloning of a novel retinoic-acid metabolizing cytochrome P450, Cyp26B1, and comparative expression analysis with Cyp26A1 during early murine development. *Mech. Dev.* **107**, 195-201.
Maden, M. (1980). Intercalary regeneration in the amphibian limb and the rule of distal transformation. *J. Embryol. Exp. Morphol.* **56**, 201-209.
Maden, M. (1982). Vitamin A and pattern formation in the regenerating limb. *Nature* **295**, 672-675.
Maden, M. (1983). The effect of vitamin A on the regenerating axolotl limb. *J. Embryol. Exp. Morphol.* **77**, 273-295.
Maden, M. (1998). Retinoids as endogenous components of the regenerating limb and tail. *Wound Repair Regen.* **6**, 358-365.
Maden, M. (2007). Retinoic acid in the development, regeneration and maintenance of the nervous system. *Nat. Rev. Neurosci.* **8**, 755-765.
Mariani, F. V., Ahn, C. P. and Martin, G. R. (2008). Genetic evidence that FGFs have an instructive role in limb proximal-distal patterning. *Nature* **453**, 401-405.
Marlétaz, F., Holland, L. Z., Laudet, V. and Schubert, M. (2006). Retinoic acid signaling and the evolution of chordates. *Int. J. Biol. Sci.* **2**, 38-47.
Maruyama, K., Kawagoe, T., Kondo, T., Akira, S. and Takeuchi, O. (2012). TRAF family member-associated NF-kappaB activator (TANK) is a negative regulator of osteoclastogenesis and bone formation. *J. Biol. Chem.* **287**, 29114-29124.
McCusker, C. D. and Gardiner, D. M. (2013). Positional information is reprogrammed in blastema cells of the regenerating limb of the axolotl (Ambystoma mexicanum). *PLoS ONE* **8**, e77064.
McCusker, C., Lehrberg, J. and Gardiner, D. (2014). Position-specific induction of ectopic limbs in non-regenerating blastemas on axolotl forelimbs. *Regeneration* **1**, 27-34.
McCusker, C. D., Athippozhy, A., Diaz-Castillo, C., Fowlkes, C., Gardiner, D. M. and Voss, S. R. (2015). Positional plasticity in regenerating Amybstoma mexicanum limbs is associated with cell proliferation and pathways of cellular differentiation. *BMC Dev. Biol.* **15**, 45.
McEwan, J., Lynch, J. and Beck, C. W. (2011). Expression of key retinoic acid modulating genes suggests active regulation during development and regeneration of the amphibian limb. *Dev. Dyn.* **240**, 1259-1270.
Mercader, N., Leonardo, E., Piedra, M. E., Martínez-A, C., Ros, M. A. and Torres, M. (2000). Opposing RA and FGF signals control proximodistal vertebrate limb development through regulation of Meis genes. *Development* **127**, 3961-3970.
Mercader, N., Tanaka, E. M. and Torres, M. (2005). Proximodistal identity during vertebrate limb regeneration is regulated by Meis homeodomain proteins. *Development* **132**, 4131-4142.
Merzdorf, C. S. (2007). Emerging roles for zic genes in early development. *Dev. Dyn.* **236**, 922-940.
Minowada, G., Jarvis, L. A., Chi, C. L., Neubuser, A., Sun, X., Hacohen, N., Krasnow, M. A. and Martin, G. R. (1999). Vertebrate Sprouty genes are induced by FGF signaling and can cause chondrodysplasia when overexpressed. *Development* **126**, 4465-4475.
Monaghan, J. R. and Maden, M. (2012a). Cellular plasticity during vertebrate appendage regeneration. *Curr. Top. Microbiol. Immunol.* **367**, 53-74.
Monaghan, J. R. and Maden, M. (2012b). Visualization of retinoic acid signaling in transgenic axolotls during limb development and regeneration. *Dev. Biol.* **368**, 63-75.
Monaghan, J. R., Epp, L. G., Putta, S., Page, R. B., Walker, J. A., Beachy, C. K., Zhu, W., Pao, G. M., Verma, I. M., Hunter, T. et al. (2009). Microarray and cDNA sequence analysis of transcription during nerve-dependent limb regeneration. *BMC Biol.* **7**, 1.
Monaghan, J. R., Athippozhy, A., Seifert, A. W., Putta, S., Stromberg, A. J., Maden, M., Gardiner, D. M. and Voss, S. R. (2012). Gene expression patterns specific to the regenerating limb of the Mexican axolotl. *Biol. Open* **1**, 937-948.
Nacu, E., Glausch, M., Le, H. Q., Damanik, F. F. R., Schuez, M., Knapp, D., Khattak, S., Richter, T. and Tanaka, E. M. (2013). Connective tissue cells, but not muscle cells, are involved in establishing the proximo-distal outcome of limb regeneration in the axolotl. *Development* **140**, 513-518.
Nacu, E., Gromberg, E., Oliveira, C. R., Drechsel, D. and Tanaka, E. M. (2016). FGF8 and SHH substitute for anterior-posterior tissue interactions to induce limb regeneration. *Nature* **533**, 407-410.
Nardi, J. B. and Stocum, D. L. (1984). Surface properties of regenerating limb cells: evidence for gradation along the proximodistal axis. *Differentiation* **25**, 27-31.
Niazi, I. A., Pescitelli, M. J. and Stocum, D. L. (1985). Stage-dependent effects of retinoic acid on regenerating urodele limbs. *Wilhelm Roux's Arch. Dev. Biol.* **194**, 355-363.
Niederreither, K., Vermot, J., Schuhbaur, B., Chambon, P. and Dollé, P. (2002). Embryonic retinoic acid synthesis is required for forelimb growth and anteroposterior patterning in the mouse. *Development* **129**, 3563-3574.
Nimura, K., Ura, K., Shiratori, H., Ikawa, M., Okabe, M., Schwartz, R. J. and Kaneda, Y. (2009). A histone H3 lysine 36 trimethyltransferase links Nkx2-5 to Wolf-Hirschhorn syndrome. *Nature* **460**, 287-291.
Nye, H. L. D., Cameron, J. A., Chernoff, E. A. G. and Stocum, D. L. (2003). Extending the table of stages of normal development of the axolotl: limb development. *Dev. Dyn.* **226**, 555-560.
O'Connor, J. P., Manigrasso, M. B., Kim, B. D. and Subramanian, S. (2014). Fracture healing and lipid mediators. *BoneKEy Rep.* **3**, 517.
Patel, N., Khan, A. O., Mansour, A., Mohamed, J. Y., Al-Assiri, A., Haddad, R., Jia, X., Xiong, Y., Mégarbané, A., Traboulsi, E. I. et al. (2014). Mutations in ASPH cause facial dysmorphism, lens dislocation, anterior-segment abnormalities, and spontaneous filtering blebs, or Traboulsi syndrome. *Am. J. Hum. Genet.* **94**, 755-759.

Pecorino, L. T., Entwistle, A. and Brockes, J. P. (1996). Activation of a single retinoic acid receptor isoform mediates proximodistal respecification. *Curr. Biol.* **6**, 563-569.
Pennimpede, T., Cameron, D. A., MacLean, G. A. and Petkovich, M. (2010). Analysis of Cyp26b1/Rarg compound-null mice reveals two genetically separable effects of retinoic acid on limb outgrowth. *Dev. Biol.* **339**, 179-186.
Phan, A. Q., Lee, J., Oei, M., Flath, C., Hwe, C., Mariano, R., Vu, T., Shu, C., Dinh, A., Simkin, J. et al. (2015). Position information in axolotl and mouse limb ECM is mediated via heparin sulfates and FGF during limb regeneration in the Axolotl (Ambystoma mexicanum). *Regeneration* **2**, 182-201.
Pietsch, P. (1993). Retinoic acid treatment inhibits mitosis in the pre-existing spinal cord during tail regeneration of the axolotl larva, Ambystoma mexicanum. *Cytobios* **76**, 7-11.
Ragsdale, C. W., Jr, Petkovich, M., Gates, P. B., Chambon, P. and Brockes, J. P. (1989). Identification of a novel retinoic acid receptor in regenerative tissues of the newt. *Nature* **341**, 654-657.
Ristevski, S., Tam, P. P. L., Kola, I. and Hertzog, P. (2001). Desrt, an AT-rich interaction domain family transcription factor gene, is an early marker for nephrogenic mesoderm and is expressed dynamically during mouse limb development. *Mech. Dev.* **104**, 139-142.
Ritchie, M. E., Phipson, B., Wu, D., Hu, Y., Law, C. W., Shi, W. and Smyth, G. K. (2015). limma powers differential expression analyses for RNA-sequencing and microarray studies. *Nucleic Acids Res.* **43**, e47.
Rochette-Egly, C. and Germain, P. (2009). Dynamic and combinatorial control of gene expression by nuclear retinoic acid receptors (RARs). *Nucl. Recept. Signal.* **7**, e005.
Roensch, K., Tazaki, A., Chara, O. and Tanaka, E. M. (2013). Progressive specification rather than intercalation of segments during limb regeneration. *Science* **342**, 1375-1379.
Roselló-Díez, A., Ros, M. A. and Torres, M. (2011). Diffusible signals, not autonomous mechanisms, determine the main proximodistal limb subdivision. *Science* **332**, 1086-1088.
Rosello-Diez, A., Arques, C. G., Delgado, I., Giovinazzo, G. and Torres, M. (2014). Diffusible signals and epigenetic timing cooperate in late proximo-distal limb patterning. *Development* **141**, 1534-1543.
Saldanha, A. J. (2004). Java Treeview–extensible visualization of microarray data. *Bioinformatics* **20**, 3246-3248.
Sandell, L. L., Sanderson, B. W., Moiseyev, G., Johnson, T., Mushegian, A., Young, K., Rey, J.-P., Ma, J.-X., Staehling-Hampton, K. and Trainor, P. A. (2007). RDH10 is essential for synthesis of embryonic retinoic acid and is required for limb, craniofacial, and organ development. *Genes Dev.* **21**, 1113-1124.
Sandell, L. L., Lynn, M. L., Inman, K. E., McDowell, W. and Trainor, P. A. (2012). RDH10 oxidation of Vitamin A is a critical control step in synthesis of retinoic acid during mouse embryogenesis. *PLoS ONE* **7**, e30698.
Scadding, S. R. (2000). Citral, an inhibitor of retinoic acid synthesis, modifies pattern formation during limb regeneration in the axolotl Ambystoma mexicanum. *Can. J. Zool.* **77**, 1835-1837.
Scadding, S. R. and Maden, M. (1986). Comparison of the effects of vitamin A on limb development and regeneration in the axolotl, Ambystoma mexicanum. *J. Embryol. Exp. Morphol.* **91**, 19-34.
Scadding, S. R. and Maden, M. (1994). Retinoic acid gradients during limb regeneration. *Dev. Biol.* **162**, 608-617.
Scotti, M., Kherdjemil, Y., Roux, M. and Kmita, M. (2015). A Hoxa13:Cre mouse strain for conditional gene manipulation in developing limb, hindgut, and urogenital system. *Genesis* **53**, 366-376.
Selleri, L., Depew, M. J., Jacobs, Y., Chanda, S. K., Tsang, K. Y., Cheah, K. S., Rubenstein, J. L., O'Gorman, S. and Cleary, M. L. (2001). Requirement for Pbx1 in skeletal patterning and programming chondrocyte proliferation and differentiation. *Development* **128**, 3543-3557.
Semba, K., Araki, K., Li, Z., Matsumoto, K.-I., Suzuki, M., Nakagata, N., Takagi, K., Takeya, M., Yoshinobu, K., Araki, M. et al. (2006). A novel murine gene, sickle tail, linked to the Danforth's short tail locus, is required for normal development of the intervertebral disc. *Genetics* **172**, 445-456.
Shimono, K., Morrison, T. N., Tung, W.-E., Chandraratna, R. A., Williams, J. A., Iwamoto, M. and Pacifici, M. (2010). Inhibition of ectopic bone formation by a selective retinoic acid receptor alpha-agonist: a new therapy for heterotopic ossification? *J. Orthop. Res.* **28**, 271-277.
Shimono, K., Tung, W.-E., Macolino, C., Chi, A. H.-T., Didizian, J. H., Mundy, C., Chandraratna, R. A., Mishina, Y., Enomoto-Iwamoto, M., Pacifici, M. et al. (2011). Potent inhibition of heterotopic ossification by nuclear retinoic acid receptor-γ agonists. *Nat. Med.* **17**, 454-460.
Simon, H. G. and Tabin, C. J. (1993). Analysis of Hox-4.5 and Hox-3.6 expression during newt limb regeneration: differential regulation of paralogous Hox genes suggest different roles for members of different Hox clusters. *Development* **117**, 1397-1407.
Smith, C. M., Finger, J. H., Hayamizu, T. F., McCright, I. J., Xu, J., Berghout, J., Campbell, J., Corbani, L. E., Forthofer, K. L., Frost, P. J. et al. (2014). The mouse Gene Expression Database (GXD): 2014 update. *Nucleic Acids Res.* **42**, D818-D824.
Stocum, D. L. and Cameron, J. A. (2011). Looking proximally and distally: 100 years of limb regeneration and beyond. *Dev. Dyn.* **240**, 943-968.
Stocum, D. L. and Thoms, S. D. (1984). Retinoic-acid-induced pattern completion in regenerating double anterior limbs of urodeles. *J. Exp. Zool.* **232**, 207-215.
Stratford, T., Horton, C. and Maden, M. (1996). Retinoic acid is required for the initiation of outgrowth in the chick limb bud. *Curr. Biol.* **6**, 1124-1133.
Suzuki, D., Yamada, A. and Kamijo, R. (2013). The essential roles of the small GTPase Rac1 in limb development. *J. Oral Biosci.* **55**, 116-121.
Taher, L., Collette, N. M., Murugesh, D., Maxwell, E., Ovcharenko, I. and Loots, G. G. (2011). Global gene expression analysis of murine limb development. *PLoS ONE* **6**, e28358.
Torchia, J., Rose, D. W., Inostroza, J., Kamei, Y., Westin, S., Glass, C. K. and Rosenfeld, M. G. (1997). The transcriptional co-activator p/CIP binds CBP and mediates nuclear-receptor function. *Nature* **387**, 677-684.
Tribioli, C., Robledo, R. F. and Lufkin, T. (2002). The murine fork head gene Foxn2 is expressed in craniofacial, limb, CNS and somitic tissues during embryogenesis. *Mech. Dev.* **118**, 161-163.
Tzchori, I., Day, T. F., Carolan, P. J., Zhao, Y., Wassif, C. A., Li, L., Lewandoski, M., Gorivodsky, M., Love, P. E., Porter, F. D. et al. (2009). LIM homeobox transcription factors integrate signaling events that control three-dimensional limb patterning and growth. *Development* **136**, 1375-1385.
Voss, S. R., Palumbo, A., Nagarajan, R., Gardiner, D. M., Muneoka, K., Stromberg, A. J. and Athippozhy, A. T. (2015). Gene expression during the first 28 days of axolotl limb regeneration I: experimental design and global analysis of gene expression. *Regeneration* **2**, 120-136.
Wakahara, T., Kusu, N., Yamauchi, H., Kimura, I., Konishi, M., Miyake, A. and Itoh, N. (2007). Fibin, a novel secreted lateral plate mesoderm signal, is essential for pectoral fin bud initiation in zebrafish. *Dev. Biol.* **303**, 527-535.
Wang, Y.-H. and Beck, C. W. (2014). Distal expression of sprouty (spry) genes during Xenopus laevis limb development and regeneration. *Gene Expr. Patterns* **15**, 61-66.
Weston, A. D., Chandraratna, R. A. S., Torchia, J. and Underhill, T. M. (2002). Requirement for RAR-mediated gene repression in skeletal progenitor differentiation. *J. Cell Biol.* **158**, 39-51.
Weston, A. D., Blumberg, B. and Underhill, T. M. (2003a). Active repression by unliganded retinoid receptors in development: less is sometimes more. *J. Cell Biol.* **161**, 223-228.
Weston, A. D., Hoffman, L. M. and Underhill, T. M. (2003b). Revisiting the role of retinoid signaling in skeletal development. *Birth Defects Res. C Embryo Today* **69**, 156-173.
Williams, J. A., Kondo, N., Okabe, T., Takeshita, N., Pilchak, D. M., Koyama, E., Ochiai, T., Jensen, D., Chu, M.-L., Kane, M. A. et al. (2009). Retinoic acid receptors are required for skeletal growth, matrix homeostasis and growth plate function in postnatal mouse. *Dev. Biol.* **328**, 315-327.
Yang, E. V., Gardiner, D. M., Carlson, M. R. J., Nugas, C. A. and Bryant, S. V. (1999). Expression of Mmp-9 and related matrix metalloproteinase genes during axolotl limb regeneration. *Dev. Dyn.* **216**, 2-9.
Yashiro, K., Zhao, X., Uehara, M., Yamashita, K., Nishijima, M., Nishino, J., Saijoh, Y., Sakai, Y. and Hamada, H. (2004). Regulation of retinoic acid distribution is required for proximodistal patterning and outgrowth of the developing mouse limb. *Dev. Cell* **6**, 411-422.

Table S1: List of probe-sets in Clusters 1-5. Contigs V4 represents the sequence ID in the version four assembly of the axolotl transcriptome found at Salsite
Expression values are averages across four biological replicates.

Cluster 1 – ID	Contig V4	Symbol	DMSO	LE135	RA
axo08692-f_at	contig404063	CYP26A1	206.93	4942.52	6138.28
axo27297-f_at	contig318347	GATA2	29.63	346.64	256.60
axo14037-f_at	contig329187	FAM115C	56.16	592.10	413.40
axo13259-r_at	contig348431	ACAN	441.97	2591.37	2653.07
axo07326-r_at	contig218026	GMDS	104.31	686.30	624.33
axo18217-r_at	contig348431	BCAN	215.36	1126.55	1287.46
axo08053-f_at	contig141405	KRT15	300.37	1373.52	1465.14
axo08185-f_at	contig122752	MMP13	208.99	578.21	706.94
axo03439-f_at	contig315788	EFEMP1	80.16	295.59	270.68
axo10102-r_at	contig96550	FAP	281.57	721.34	831.81
axo31468-f_at	contig182995	B3GNT5	130.45	321.26	371.32
axo04609-f_at	contig317411	NLRP12	42.01	116.74	113.19
axo08054-f_at	contig71066	KRT19	9658.14	27560.78	25675.97
axo08051-f_at	contig327242	KRT15	155.29	481.81	401.88
axo24095-f_at	contig214059	KRT8	575.91	1289.14	1420.97
axo07862-r_at	contig335606	GCG	31.81	68.22	78.45
axo17107-f_at	contig336912	DSCR6	16.72	40.66	40.45
axo25693-f_at	contig201477	TGM2	652.45	1468.78	1561.64
axo28644-f_at	contig203883	ALPL	122.24	335.71	287.30
axo15578-f_s_at	contig81812	A4GNT	431.26	970.64	1013.45
axo07680-f_at	contig91429	CRABP2	3289.69	6610.13	7545.86
axo25211-f_at	contig315732	0	300.71	749.00	666.44
axo27294-f_at	contig315750	BHLHE40	378.89	899.77	809.40
axo23402-f_at	contig183596	CES2	99.34	187.38	207.68
axo05908-f_at	contig209094	ASL	722.72	1606.02	1492.71
axo07733-f_at	contig320648	DPP4	109.84	226.50	226.33
axo07976-r_at	contig131595	ALDH1A3	683.05	1636.81	1391.14
axo30225-f_at	contig314469	ELF3	1654.97	3676.45	3359.76
axo19762-f_at	contig188679	DSEL	49.98	115.32	98.66
axo05722-r_at	contig323717	ELFN1	101.09	177.15	196.24
axo08049-f_at	contig214059	KRT8	5986.20	10357.20	11238.32
axo09472-r_at	contig319793	SLC4A4	61.84	127.43	115.60
axo14467-f_at	contig315430	SWAP70	19.71	34.45	36.43
axo05068-f_at	contig318764	CYP4B1	625.50	1091.98	1148.85
axo08615-r_at	contig317111	CYP2C8	207.74	392.39	379.66
axo11396-f_at	contig333619	TM6SF2	315.16	572.31	569.35
axo11397-f_at	contig333619	TM6SF2	220.15	387.67	388.74
axo03338-r_at	contig317491	CDC42SE2	485.66	950.48	851.72
axo17564-f_at	contig317525	NAV1	165.45	302.21	289.09
axo12218-f_at	contig314480	VIL1	253.52	442.71	433.44
axo25795-f_at	contig318372	0	464.86	792.02	792.20
axo29912-f_at	contig139769	TNFRSF1B	22.61	39.51	38.34
axo17498-f_at	contig183147	ABI1	1387.95	2104.84	2241.23
axo05837-f_at	contig203116	MYO1B	1298.48	2165.57	2089.55
axo16547-r_at	contig122366	FAM102B	280.72	433.82	450.16
axo08834-f_at	contig140063	SOAT1	255.94	390.27	408.64
axo26974-f_at	contig320054	0	16.82	26.55	26.48
axo19900-f_at	contig315542	FBLIM1	434.87	738.42	678.83
axo30108-f_at	contig314620	0	41.89	61.70	63.02
axo11599-f_at	contig94773	VPS72	17.65	26.57	26.48
axo26087-f_at	contig134905	0	501.02	757.08	714.95
axo01417-r_at	contig327148	GORAB	29.41	44.97	41.81

Cluster 1 – ID	Contig V4	Symbol	DMSO	LE135	RA
axo07075-r_at	contig02839	CIRBP	3087.57	5578.40	3505.32
axo29369-f_at	contig183228	LOC100497968	122.14	256.69	161.88
axo24161-r_at	contig204290	0	53.96	112.11	74.22
axo24313-f_at	contig100963	B4GALT3	51.57	180.95	120.88
axo29536-f_at	contig314545	SP7	133.59	384.16	256.79
axo12983-r_at	contig335498	EHF	826.37	1966.11	1343.34
axo30265-f_at	contig183227	LOC100497968	49.61	105.24	74.58
axo08789-f_at	contig317911	SLC9A2	85.56	162.48	115.91
axo21124-f_at	contig315674	SGK2	282.70	596.25	426.51
axo03617-f_at	contig324495	HTR3A	34.46	57.45	41.64
axo06308-r_at	contig354267	HSBP1L1	41.02	135.84	98.68
axo09488-f_at	contig100960	B4GALT3	955.28	2999.29	2201.87
axo12430-r_at	contig320049	UGT2A1	788.16	1694.39	1263.26
axo30867-f_at	contig317945	ORF2p	373.85	567.49	423.43
axo07918-r_at	contig324756	ALDH1A1	347.57	562.09	430.02
axo01703-f_at	contig314545	SP7	196.49	323.57	249.27
axo17370-f_at	contig314941	C1GALT1	368.24	861.70	669.21
axo12581-f_at	contig330612	UPK3A	238.40	509.81	397.74
axo12451-f_at	contig94841	ANXA2	424.67	704.58	552.16
axo02833-r_at	contig144380	DLGAP4	59.05	129.24	102.07
axo26457-f_at	contig87521	UPK2	2297.17	3588.20	2843.95
axo07299-f_at	contig89851	FLT3LG	189.88	321.81	255.19
axo13799-f_at	contig158933	SMPDL3B	342.62	905.37	727.38
axo22098-r_at	contig317558	LOC582826	3847.70	8269.39	6701.24
axo29553-f_at	contig42357	0	400.84	717.91	584.15
axo08960-f_at	contig96781	TGFB2	301.57	555.90	452.67
axo05154-f_at	contig41026	0	724.64	1422.61	1158.55
axo17801-f_at	contig156665	BCAM	254.59	403.02	334.21
axo27969-f_at	contig314941	C1GALT1	139.14	273.43	231.55
axo11787-f_at	contig61273	NNMT	74.74	152.63	129.42
axo06338-r_at	contig156177	ALOX15B	133.36	238.97	203.02
axo19070-f_at	contig203757	TMC7	99.94	151.28	130.48
axo01377-r_at	contig191125	CYB5A	76.52	129.18	112.19
axo12781-r_at	contig317883	DUSP10	75.81	126.90	111.28
axo09834-r_at	contig331211	PLCB3	41.01	67.21	59.35
axo17095-r_at	contig325397	HOXC5	292.80	493.18	437.38
axo19887-f_at	contig315542	FBLIM1	640.27	1043.58	929.60
axo00636-f_at	contig183192	TANK	879.69	1444.06	1286.95
axo08707-r_at	contig317059	CYP27A1	33.92	53.63	48.04
axo06339-f_at	contig284820	ALOXE3	3087.57	5578.40	3505.32
axo25438-f_at	contig315060	LOC100487575	122.14	256.69	161.88
axo01819-f_at	contig325945	TMEM86A	53.96	112.11	74.22
axo03393-f_at	contig124564	PDLIM7	51.57	180.95	120.88
axo19069-f_at	contig203757	TMC7	133.59	384.16	256.79
axo26981-f_at	contig323649	0	826.37	1966.11	1343.34
Cluster 2 – ID	**Contig V4**	**Symbol**	**DMSO**	**LE135**	**RA**
axo08368-f_at	contig213508	SERPINF1	2222.93	2615.88	3353.78
axo02065-f_at	contig222675	PAPLN	52.57	64.65	81.43
axo13076-f_at	contig314961	TLK1	116.40	143.46	190.70
axo00939-f_at	contig201534	AP2B1	116.71	144.40	190.34
axo30735-f_at	contig1150716	0	13.11	16.25	22.63
axo05737-r_at	contig89831	SRRT	268.94	336.86	407.11
axo04940-f_at	contig160920	KIAA1217	93.68	117.44	153.39
axo02837-f_at	contig183029	ZMYND8	66.84	84.41	108.94
axo13263-f_at	contig319754	FLRT2	312.86	397.29	495.56

axo10840-f_at	contig58983	PTBP3	209.23	267.25	351.83
axo20348-f_s_at	contig02585	0	9769.92	12530.66	15647.45
axo20225-f_at	contig70850	SYTL2	212.70	273.22	347.32
axo12449-f_at	contig145163	PDIA5	34.12	44.18	55.01
axo09815-f_at	contig201539	CLN3	33.92	43.99	52.21
axo10279-f_at	contig201438	RARG	404.54	527.35	655.00
axo21749-f_at	contig44885	ASPH	198.17	259.33	300.95
axo13945-f_at	contig519847	LPIN2	49.35	65.61	100.91
axo10841-r_at	contig344288	ABL1	55.78	74.22	91.60
axo19786-f_at	contig201354	ARID5B	27.97	37.28	59.74
axo02482-f_at	contig201352	SPTBN1	26.95	36.00	52.65
axo08278-f_at	contig84092	NEO1	115.05	155.30	186.05
axo17170-f_at	contig317767	TMX3	145.57	196.60	221.16
axo01916-f_at	contig204125	MEIS1	897.36	1212.16	1785.85
axo24728-f_at	contig316121	Pbx1	395.06	534.52	700.85
axo07972-f_at	contig75853	IL6ST	57.63	78.14	88.18
axo03303-r_at	contig913319	ZNF644	60.32	82.40	94.17
axo10988-r_at	contig78881	HDLBP	1420.33	1943.08	2547.26
axo02500-f_at	contig321365	FAM83C	194.22	266.91	297.16
axo09449-f_at	contig316562	EIF3A	445.80	616.76	746.79
axo22373-f_at	contig316018	ELL	53.29	74.14	95.44
axo27168-f_at	contig202564	0	238.22	335.72	391.76
axo18098-f_at	contig314341	SCAF1	280.16	395.16	448.53
axo19270-r_at	contig316018	ELL	101.26	143.42	189.34
axo31446-f_at	contig498950	0	50.94	73.87	108.31
axo09451-f_at	contig316562	EIF3A	634.16	931.40	1229.75
axo06511-f_at	contig206427	PCDH15	15.66	23.33	33.83
axo15793-f_at	contig316735	PLEK2	166.06	248.29	408.61
axo12547-f_at	contig31793	RAC1	701.66	1064.01	1181.86
axo08165-f_at	contig204123	MEIS2	137.27	208.44	264.12
axo01066-f_at	contig183103	DHRS13	81.29	123.44	146.07
axo12021-r_at	contig208666	PAMR1	318.53	484.30	840.24
axo31342-f_at	contig07038	MDK	167.61	255.19	329.75
axo15637-f_at	contig232269	RBPMS	77.73	118.36	167.40
axo23856-r_at	contig314286	ZNF638	96.62	147.26	215.29
axo23411-r_at	contig350226	12-RFa	60.98	94.83	118.88
axo13184-f_at	contig314239	PLXNB2	100.29	156.09	198.67
axo01242-f_at	contig314311	B3GNT7	46.45	72.35	101.10
axo22164-f_at	contig319202	ORF2p	130.36	205.95	241.33
axo23774-r_at	contig98141	SAMD9L	83.61	135.11	167.95
axo31529-f_at	contig609088	0	97.10	158.29	249.21
axo08144-f_at	contig324772	MAS1	139.57	227.68	341.54
axo02272-r_at	contig314591	KAL1	75.40	129.78	253.14
axo26463-f_at	contig11072	0	342.25	590.31	887.54
axo29897-f_at	contig202141	0	49.03	88.16	163.80
axo02614-f_at	contig156685	NCOA3	38.38	69.85	90.50
axo08659-f_at	contig348569	RBP1	141.66	258.82	476.33
axo07968-f_at	contig331042	IGFBP6	118.06	217.57	379.44
axo09525-f_at	contig201630	ADAM9	84.50	171.31	202.24
axo03112-r_at	contig202866	MIA3	64.50	131.75	157.92
axo12406-f_at	contig325335	INMT	121.14	252.11	347.90
axo00883-r_at	contig201901	SDR16C5	72.08	152.16	213.62
axo05624-r_at	contig202985	PAX6	70.22	149.63	244.68
axo19711-f_at	contig182995	B3GNT5	602.57	1323.91	1677.55
axo17540-f_at	contig32472	RHBG	128.26	309.64	409.04
axo15713-f_at	contig32473	0	203.57	509.54	794.09

axo17320-f_at	contig314231	CYP26B1	140.39	385.65	787.24
axo10419-r_at	contig319441	DHRS3	1248.15	3909.38	5533.37
Cluster 3 – ID	**Contig V4**	**Symbol**	**DMSO**	**LE135**	**RA**
axo01795-f_at	contig317829	COL6A6	34.91	53.71	131.57
axo07673-f_at	contig317221	TGFB1	582.86	854.03	1921.79
axo09203-f_at	contig202959	NRIP1	295.99	403.26	759.93
axo29426-f_at	contig319614	0	45.23	59.94	154.86
axo29487-f_at	contig113456	0	267.38	352.02	685.39
axo22976-r_at	contig536857	ORF2p	40.80	53.16	91.01
axo14857-r_at	contig406348	FABP2	620.43	779.39	1572.08
axo20292-f_at	contig202171	ZNF628	29.64	37.18	60.59
axo01743-f_at	contig213606	APCDD1	440.27	549.05	935.47
axo14041-f_at	contig144299	SLK	204.39	251.61	378.62
axo12878-f_at	contig505525	ZNF236	17.77	21.70	32.37
axo10076-f_at	contig316552	EPHA7	185.71	219.25	338.68
axo10855-r_at	contig318118	RND3	670.15	788.15	1105.81
axo11498-f_at	contig144414	MAP1B	14.62	16.96	22.28
axo05508-f_at	contig108550	NAT2	54.79	63.16	105.93
axo29388-f_at	contig122394	0	65.20	74.66	185.21
axo01710-f_at	contig321423	COL24A1	47.55	54.17	78.23
axo29834-f_at	contig104866	0	20.70	23.57	32.02
axo18601-f_at	contig314286	ZNF638	152.37	170.92	263.03
axo21619-f_at	contig79033	MUC17	35.75	39.94	54.32
axo08089-r_at	contig144601	LGALS9	2679.95	2991.92	4555.10
axo02086-f_at	contig318355	TSHZ2	225.46	251.29	346.67
axo06130-f_at	contig00844	DCTN1	37.72	41.79	60.10
axo08887-f_at	contig314230	STAT3	23.69	26.24	39.09
axo22289-f_at	contig492717	0	17.01	18.76	28.94
axo22862-f_at	contig572444	NR3C1	101.51	110.35	167.44
axo07689-f_at	contig108550	NAT2	44.13	47.69	87.20
axo07751-r_at	contig203287	EDNRA	519.21	558.64	907.72
axo21366-f_at	contig449042	HTRA3	26.13	27.60	39.40
axo05907-r_at	contig29809	ERVW-1	150.00	157.05	261.95
axo19156-f_x_at	contig522203	PIF1	61.29	63.89	108.11
axo03396-r_at	contig324586	FIBIN	69.68	70.56	127.29
axo04567-r_at	contig318000	TLL2	152.60	145.73	242.09
axo08870-f_at	contig319633	CETP	104.43	90.74	228.96
Cluster 4 – ID	**Contig V4**	**Symbol**	**DMSO**	**LE135**	**RA**
axo17416-r_at	contig328693	LHX9	240.73	205.15	86.37
axo21354-f_at	contig459992	ZIC5	39.14	33.58	15.20
axo08094-f_at	contig215586	LMO1	192.22	196.26	60.33
axo10448-r_at	contig329813	LHX2	341.74	348.14	140.28
axo08686-r_at	contig326664	RGS2	3359.06	3377.30	2092.44
axo03262-f_at	contig323589	SPRY1	367.20	367.57	218.05
axo06661-f_at	contig109796	CLEC4M	122.22	120.89	77.77
axo00475-f_at	contig204667	RGS18	225.73	222.16	147.76
axo02727-f_at	contig183419	VSTM2A	51.68	55.35	26.16
axo08208-f_at	contig327908	MSX2	156.71	167.21	93.40
axo17093-f_at	contig324990	ERRFI1	185.56	222.43	110.74
axo00912-f_at	contig205530	DNER	136.25	167.57	63.95
axo06766-f_at	contig446525	HOXA13	22.01	32.11	12.79
axo08047-r_at	contig104978	ALOX5	29.13	45.27	24.89
Cluster 5 – ID	**Contig V4**	**Symbol**	**DMSO**	**LE135**	**RA**
axo09539-f_at	contig317419	MATN4	1348.80	373.08	155.82
axo27453-f_at	contig316336	SOX8	313.38	227.52	121.60
axo12750-f_at	contig319644	PRSS23	564.03	341.49	196.12

axo15048-r_at	contig322672	SOSTDC1	255.65	204.55	117.99
axo21673-f_at	contig400485	PLAUR	179.45	91.64	54.58
axo10418-f_at	contig213430	CRLF1	1079.79	625.61	399.22
axo16582-f_at	contig324910	DOK4	311.50	101.27	65.46
axo00390-f_at	contig329351	ACY3	814.29	495.42	320.89
axo15307-f_at	contig35781	PRLH	335.21	104.07	69.31
axo12311-f_at	contig146295	CYP46A1	73.31	58.52	40.01
axo15597-f_at	contig332528	TMEFF2	74.85	59.79	41.27
axo05010-f_at	contig331193	ODZ4	23.45	16.84	11.78
axo19810-r_at	contig315011	SLITRK6	916.05	713.99	514.51
axo08991-f_at	contig317515	TLR2	235.53	146.54	110.78
axo21139-f_at	contig315752	FAM198A	300.85	255.04	196.46
axo31298-f_at	contig125174	SRSF1	71.71	51.32	39.67
axo11178-r_at	contig322738	KRT6A	8101.74	4824.81	3763.45
axo10111-f_at	contig328429	FIGF	149.24	113.90	89.32
axo25678-f_at	contig321552	0	122.86	75.87	59.78
axo18649-f_at	contig320823	ADRB2	157.53	121.28	98.70
axo17132-f_at	contig333290	GFOD1	568.41	456.51	371.87
axo10575-f_at	contig00360	AQP3	459.94	171.16	140.57
axo00180-f_at	contig316890	HK2	1853.51	1472.50	1212.80
axo29026-f_at	contig315244	EBF3	46.40	21.60	17.88
axo17962-r_at	contig315424	SNTB1	367.74	243.29	202.39
axo09980-f_at	contig84702	CAMP	23.72	16.93	14.21
axo16967-f_at	contig315401	LGR4	550.17	421.69	357.33
axo19489-f_at	contig326451	PPP1R14C	105.93	59.23	50.76
axo13629-r_at	contig314946	TDRD7	266.38	193.03	165.65
axo02549-r_at	contig145113	LRRTM1	29.30	21.26	18.42
axo08844-f_at	contig108643	UAP1	1225.18	648.17	565.39
axo08425-f_at	contig901913	PMCH	87.79	45.11	39.37
axo09479-r_at	contig207957	STX11	141.04	104.51	93.20
axo13728-f_at	contig145817	GPR160	1091.97	775.00	694.95
axo29537-f_at	contig00360	AQP3	4582.77	1780.67	1600.77
axo07606-f_at	contig119883	CDO1	1160.52	621.33	563.83
axo10890-f_at	contig210025	DLX6	301.14	122.98	112.94
axo09755-f_at	contig240523	DDIT3	695.84	329.48	305.58
axo28206-f_at	contig189635	0	77.07	54.73	51.22
axo09572-f_at	contig314779	NRP1	940.21	553.61	519.33
axo10235-r_at	contig145583	PPP2R2B	53.95	36.57	34.35
axo00370-r_at	contig205164	WFDC8	5302.31	2195.22	2129.59
axo01691-r_at	contig155714	MAP7D2	952.93	638.11	623.00
axo02921-f_at	contig207363	LYPD6	115.99	72.04	72.24
axo30782-f_at	contig586298	0	447.94	110.51	111.93
axo08845-f_at	contig108639	UAP1	2137.26	1051.17	1074.54
axo14878-f_at	contig213396	IFRD1	748.41	467.82	479.04
axo17826-f_at	contig315002	LRRN1	181.59	117.37	120.80
axo18334-f_at	contig224374	EPB41L4A	185.79	105.49	112.64
axo27196-f_at	contig140511	0	525.96	323.28	346.27
axo13696-f_at	contig206805	B4GALT1	217.43	138.70	149.23
axo18652-f_at	contig335278	GPR87	135.39	69.80	75.29
axo12916-f_at	contig315308	ATF5	790.21	502.27	546.94
axo29526-f_at	contig315308	ATF5	1796.67	1092.27	1191.86
axo05994-f_at	contig322028	DSG1	81.37	33.47	36.62
axo04822-f_at	contig324687	AADAC	120.96	74.05	81.51
axo30262-f_at	contig201678	POF1B	3567.33	2330.98	2572.29
axo25307-f_at	contig157229	ARHGEF3	707.56	399.07	441.12
axo30681-f_at	contig170203	0	615.84	239.19	264.87

axo07343-r_at	contig322127	IGFBP2	1676.10	850.29	945.17
axo06462-f_at	contig318299	HMMR	303.73	195.57	217.63
axo31319-f_s_at	contig340923	0	5632.84	2404.49	2703.39
axo12982-f_at	contig210232	LPAR3	709.16	470.45	530.52
axo00523-f_at	contig314561	WHSC1	117.01	74.81	84.51
axo01274-f_at	contig204252	SLC25A43	240.35	157.67	179.81
axo25163-f_at	contig31030	KRT14	202.97	74.82	85.54
axo19313-f_at	contig117893	TRAF3IP3	319.47	199.47	228.71
axo15598-f_at	contig101335	KIF20B	487.38	309.69	355.35
axo21628-f_at	contig325197	NEFH	145.25	64.20	74.43
axo24800-f_at	contig158133	0	124.89	65.62	76.17
axo06250-f_at	contig318656	TMEM2	273.92	165.18	193.54
axo10520-f_at	contig317794	KIF23	136.12	84.26	99.03
axo05362-f_at	contig101264	TGM1	1184.62	376.88	443.15
axo12794-r_at	contig320288	CA5B	6937.32	3997.12	4712.54
axo08130-f_at	contig321153	MAD2L1	1172.97	742.41	882.44
axo30895-f_at	Mex_Nohits_5134_Contig_1	DSG1	289.59	55.10	65.54
axo06014-r_at	contig107129	KRT17	24345.81	15693.58	18702.37
axo25906-f_at	contig157119	LRIG1	120.87	74.48	89.01
axo17376-f_at	contig316531	SMARCAD1	1347.62	891.88	1073.84
axo13117-f_at	contig144456	KIF4A	415.11	274.64	333.41
axo22446-f_at	contig16773	0	13354.85	7533.04	9193.32
axo16976-r_at	contig345060	MCM10	155.37	101.71	125.02
axo29791-f_at	contig337266	0	456.63	261.24	325.43
axo08594-f_at	contig183016	PTPRZ1	2774.80	1405.71	1755.90
axo22465-f_at	contig361194	LOC100493186	554.85	97.36	122.04
axo16742-f_at	contig320419	NEIL3	152.62	94.93	119.18
axo16457-f_at	contig315182	FAM83B	816.57	435.76	548.62
axo24155-f_at	contig322400	VWA1	1135.92	337.39	426.38
axo10609-f_at	contig319066	DNASE1L3	763.50	247.26	312.94
axo16459-f_at	contig315182	FAM83B	743.32	420.07	537.77
axo17023-f_at	contig93627	ANLN	1046.46	618.17	793.86
axo07565-r_at	contig157680	CAPNS1	6479.59	3797.16	4896.87
axo13224-f_at	contig191649	SSBP2	36.49	23.76	30.75
axo10960-r_at	contig193055	GPR37	90.83	39.25	52.06
axo10941-f_at	contig183579	GJB5	3725.53	2198.59	2921.63
axo07098-f_at	contig320761	CLDN4	1345.88	844.35	1147.67
axo12746-f_at	contig326291	TESK1	105.89	57.87	80.49
axo12416-f_at	contig45417	CDC42EP2	354.88	211.21	294.40
axo26830-f_at	contig315102	TNFAIP2	3344.62	1762.78	2482.56
axo05416-f_at	contig90858	TP63	506.84	285.25	402.24
axo17885-f_at	contig314301	NINL	642.02	341.98	482.59
axo09083-r_at	contig315134	UGCG	2075.89	1235.60	1771.19
axo10676-f_at	contig317489	NRCAM	33.65	21.11	30.41
axo01062-f_at	contig316980	OTOA	2030.12	992.85	1434.19
axo07003-f_at	contig318791	BMPR1B	291.16	113.49	165.75
axo27884-f_at	contig317088	0	355.63	128.55	192.28
axo14381-f_at	contig190217	PDZRN3	281.81	147.21	227.66
axo26905-f_at	contig321754	0	1307.60	815.75	1287.50
axo26217-f_at	contig321024	0	235.20	105.83	167.67
axo05289-f_at	contig01876	GJB6	506.91	91.04	144.68
axo03604-f_at	contig206358	NEBL	224.83	100.94	166.29
axo12174-f_at	contig113035	TFPI2	342.73	143.51	237.98
axo12175-f_at	contig113037	TFPI2	328.64	124.95	217.41
axo21314-f_at	contig131977	KRTAP5-8	954.17	168.56	339.30
axo06032-f_at	contig316632	KRT5	1374.40	47.06	194.55